

# Multiplexed Surrogate Analysis of Glycotransferase Activity in Whole Biospecimens

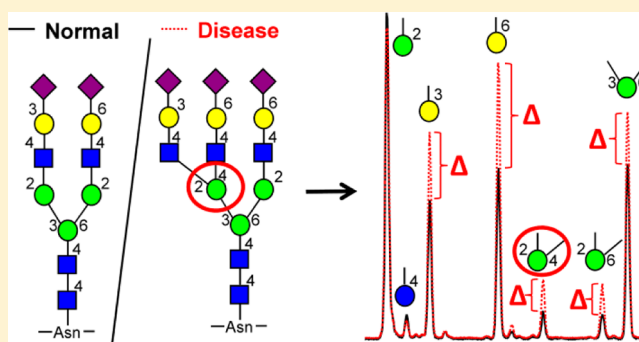
Chad R. Borges,<sup>†,\*</sup> Douglas S. Rehder,<sup>†</sup> and Paolo Boffetta<sup>‡</sup>

<sup>†</sup>Molecular Biomarkers Unit, The Biodesign Institute at Arizona State University, Tempe, Arizona 85287, United States

<sup>‡</sup>Institute for Translational Epidemiology and Tisch Cancer Institute, Mount Sinai School of Medicine, New York, New York 10029, United States

## S Supporting Information

**ABSTRACT:** Dysregulated glycotransferase enzymes in cancer cells produce aberrant glycans—some of which can help facilitate metastases. Within a cell, individual glycotransferases promiscuously help to construct dozens of unique glycan structures, making it difficult to comprehensively track their activity in biospecimens—especially where they are absent or inactive. Here, we describe an approach to deconstruct glycans in whole biospecimens then analytically pool together resulting monosaccharide-and-linkage-specific degradation products (“glycan nodes”) that directly represent the activities of specific glycotransferases. To implement this concept, a reproducible, relative quantitation-based glycan methylation analysis methodology was developed that simultaneously captures information from N-, O-, and lipid linked glycans and is compatible with whole biofluids and homogenized tissues; in total, over 30 different glycan nodes are detectable per gas chromatography–mass spectrometry (GC-MS) run. Numerous nonliver organ cancers are known to induce the production of abnormally glycosylated serum proteins. Thus, following analytical validation, in blood plasma, the technique was applied to a group of 59 lung cancer patient plasma samples and age/gender/smoking-status-matched non-neoplastic controls from the Lung Cancer in Central and Eastern Europe (CEE) study to gauge the clinical utility of the approach toward the detection of lung cancer. Ten smoking-independent glycan node ratios were found that detect lung cancer with individual receiver operating characteristic (ROC) c-statistics ranging from 0.76 to 0.88. Two glycan nodes provided novel evidence for altered ST6Gal-I and GnT-IV glycotransferase activities in lung cancer patients. In summary, a conceptually novel approach to the analysis of glycans in unfractionated human biospecimens has been developed that, upon clinical validation for specific applications, may provide diagnostic and/or predictive information in glycan-altering diseases.



Glycans are complex, heterogeneous biological sugar polymers generally found attached to proteins or lipids and displayed on cell and macromolecule surfaces. The construction and display of abnormal glycan structures is an established hallmark of nearly every known type of tumor cell and appears to facilitate their ability to metastasize.<sup>1</sup> In addition, there are numerous types of cancer, including ovarian,<sup>2,3</sup> prostate,<sup>4,5</sup> pancreatic,<sup>6,7</sup> liver,<sup>8,9</sup> multiple myeloma,<sup>10</sup> breast,<sup>11,12</sup> lung,<sup>13,14</sup> gastric,<sup>15,16</sup> thyroid,<sup>17</sup> and colorectal cancer,<sup>18</sup> as well as other inflammation-related diseases<sup>19,20</sup> that are able to induce aberrant glycosylation of abundant blood plasma proteins.

Glycans are created in the endoplasmic reticulum and golgi apparatus organelles by enzymes known as glycotransferases (GTs). Aberrant GT expression and/or activity is generally the immediate upstream cause of irregular glycan production.<sup>1</sup> Unfortunately, however, the ability to directly track the activity of one or more GTs in human biospecimens is technically difficult and/or generally precluded in common clinical samples where GTs tend to lose activity *ex vivo* or are simply absent.

The natural complexity and structural heterogeneity of glycans comes in part from the fact that GTs build at glycan polymer branch-points and chain link sites in a non-template-driven, first-come-first-build manner—i.e., there are no biologically embedded templates or instruction sets that drive glycan construction in a precise, well-defined manner (such as is the case with DNA and proteins). Yet, amidst this seemingly chaotic process, individual GTs generally exhibit strict donor, acceptor, and linkage specificity,<sup>21</sup> allowing for a moderate degree of consistency in routine glycan production.

When viewed across all protein and lipid substrates, the altered expression of a single GT can result in the production of a complex, heterogeneous mixture of *n* number of unique, abnormal whole-glycan structures rather than a uniformly increased expression of a single whole-glycan structure (see Figure 1). These heterogeneous mixtures of whole-glycan

Received: December 13, 2012

Accepted: January 31, 2013

Published: January 31, 2013

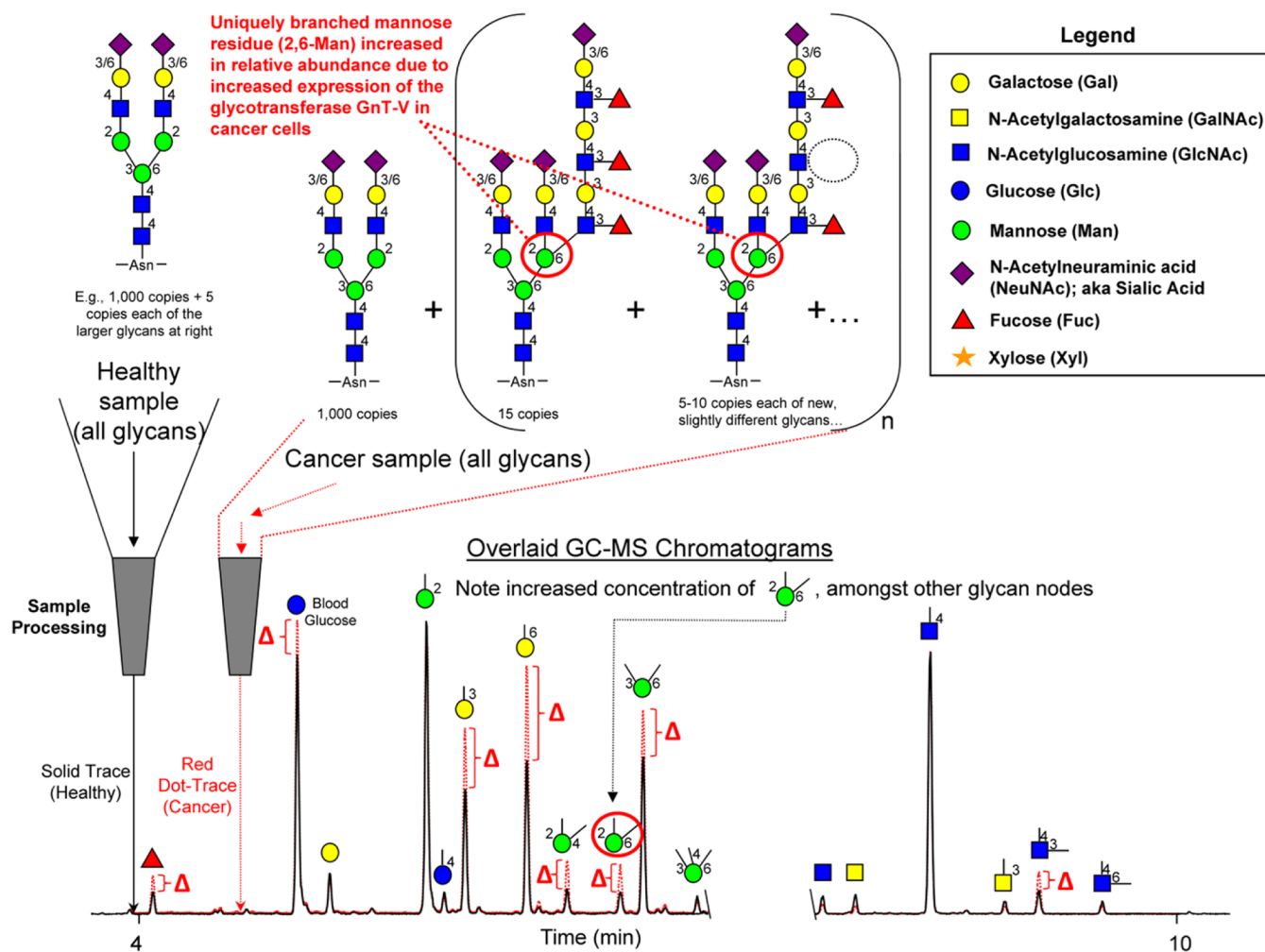


**Figure 1.** Conceptual overview of the analytical concept: An upregulated glycotransferase (GT) (e.g., GnT-V) causes an increase in the quantity of a specific, uniquely linked glycan monosaccharide residue (a 2,6-linked mannose “node” in this example)—which, through the subsequent action of other GTs, can lead to formation of a mixture of heterogeneous whole-glycan structures at low copy number each—all of which can be difficult to detect and quantify in routine fashion. Analytically pooling together the “glycan nodes” from among all the aberrant glycan structures provides a more direct surrogate measurement of GnT-V activity than any single intact glycan. Simultaneous measurement of N-, O-, and lipid linked “glycan nodes” in whole biospecimens as described here represents a conceptually novel means by which to detect and monitor glycan-affective diseases such as cancer. Actual extracted ion chromatograms from 10- $\mu$ L blood plasma samples are shown. Numbers adjacent to monosaccharide residues in glycan structures indicate the position at which the higher residue is linked to the lower residue. If no linkage positions are indicated in the chromatogram annotation, the residue is either in the terminal position or free in solution (e.g., glucose). All residues except sialic acid link downward via their 1-position; sialic acid links downward via its 2-position. The split in the chromatogram indicates the change in extracted ion chromatograms:  $m/z$  117 + 129 for hexose residues and  $m/z$  116 + 158 for N-acetylhexosamine (HexNAc) residues.

structures are difficult to fully characterize routinely—so existing cancer markers and novel candidate biomarkers that are based on intact glycan structure are generally based on one or a few particular aberrant glycan structures (out of  $n$ )—or perhaps a set of very closely related aberrant glycan structures that result in a unique antibody or lectin epitope.

With this background in mind, we developed the idea that monosaccharide-and-linkage-specific glycan polymer chain links and branch points (“glycan nodes”, as we refer to them), if broken down and quantified from the pool of all glycan structures in a biological sample, may, in numerous cases, serve as direct, 1:1 molecular surrogates of aberrant GT activity—a complementary contrast to traditional glycomics approaches that focus on the analysis of whole, intact glycans that represent 1/ $n$ :1 molecular surrogates of GT activity (Figure 1).

Below, we describe the development and technical characteristics of a clinical sample-compatible protocol by which we have

implemented this analytical concept. In the context of lung cancer, we provide an initial assessment of its utility as a methodology for routine measurement of novel glycan-based cancer markers.

## EXPERIMENTAL SECTION

**Materials.** Heavy, stable-isotope-labeled D-glucose ( $U$ - $^{13}C_6$ , 99%; 1,2,3,4,5,6-D7, 97%–98%) was obtained from Cambridge Isotope Laboratories. N-acetyl-D-[ $U$ - $^{13}C_6$ ]glucosamine and L-[ $U$ - $^{13}C_6$ ]fucose were obtained from Omicron Biochemicals, Inc. 6'-Sialyl-N-acetylglucosamine and N-acetylglucosamine were purchased from Carbosynth (U.K.). Additional monosaccharide and glycan polymer standards for verification of partially methylated alditol acetate (PMAA) identities via gas chromatography–mass spectroscopy (GC-MS) were obtained from Carbosynth, Sigma–Aldrich, V-Laboratories (which is a U.S. subsidiary of Dextra U.K.), and The Scripps Research

Institute/Consortium for Functional Glycomics. Purified proteins were obtained from EMD Millipore (Human Serum Amyloid P), Sigma–Aldrich (Bovine Ribonuclease B), and Athens Research & Technology (Human Vitamin D Binding Protein); pre-purified neutral glycosphingolipids were obtained from Enzo Life Sciences. Sodium hydroxide beads (20–40 mesh) were purchased from Sigma–Aldrich. Spin columns (0.9 mL) equipped with plugs and polyethylene frits were purchased from the Pierce division of ThermoFisher Scientific (Cat. No. 69705). GC-MS autosampler vials and Teflon-lined pierceable caps were also obtained from ThermoFisher Scientific. GC consumables were acquired from Agilent; MS consumables were obtained from Waters. All other solvents and chemicals were of the highest purity available and obtained from either ThermoFisher Scientific or Sigma–Aldrich.

**Samples.** A group of 59 blood plasma samples from lung cancer patients and age/gender/smoking-status matched controls that were enrolled in the Lung Cancer in Central and Eastern Europe (CEE) study were a gift from the International Agency for Research on Cancer Biobank in Lyon, France. Additional serum samples from nominally healthy individuals, lung cancer patients, and colorectal cancer patients were purchased from ProMedDx (Norton, MA). Serum samples from prostate cancer patients were purchased from the Cooperative Human Tissue Network (Vanderbilt, TN). Plasma samples from patients with normal glucose tolerance (NGT), impaired glucose tolerance (IGT), Type 2 diabetes (T2D), and T2D with cardiovascular disease (CVD), the latter of which is defined as a history of heart attack or stroke and/or the presence of microalbuminuria or macroalbuminuria, were provided through an ongoing NIH-sponsored collaboration with Dr. Craig Stump and Dr. Hussein Yassine, endocrinologists at the University of Arizona. (Dr. Yassine is now at the University of Southern California.) Other biospecimens were purchased from Bioreclamation (Hicksville, NY), including a 300-mL plasma sample from an individual donor, which was analyzed in every batch as a quality control sample.

**Permethylated and Semipurification of Whole Biofluid Glycans.** Permethylated and subsequent cleanup procedures were adapted from the protocol of Goetz et al.,<sup>22</sup> which was designed to permethylate and release O-linked glycans from preisolated glycoproteins. Nine microliters (9  $\mu$ L) of a whole biofluid sample (e.g., blood plasma, serum, seminal fluid, homogenized tissue, etc.) was added to a 1.5-mL polypropylene test tube. To this was added 1  $\mu$ L of an internal tracer stock solution containing 10 mM each of D-glucose ( $U\text{-}^{13}\text{C}_6$ , 99%;  $1,2,3,4,5,6,6\text{-D}_7$ , 97%–98%), N-acetyl-D-[ $UL\text{-}^{13}\text{C}_6$ ]glucosamine, and L-[ $UL\text{-}^{13}\text{C}_6$ ]fucose. (As explained below, these internal standards are useful for qualitative verification of proper sample processing, but for purposes of relative quantification, the glycan nodes within a sample are best-normalized to themselves.) To the 10- $\mu$ L sample-plus-internal-standard mixture was added 270  $\mu$ L of dimethylsulfoxide (DMSO) and 105  $\mu$ L of iodomethane. This solution was mixed thoroughly and placed onto a plugged 1-mL spin column containing  $\sim$ 0.7 g sodium hydroxide (NaOH) beads that had been preconditioned with acetonitrile, followed by two rinses with DMSO. Samples were allowed to stand for 10–12 min with occasional stirring. Samples were then unplugged and spun in a microcentrifuge for 30 s at 4000 rpm (800 g) to retrieve the glycan-containing liquid. Samples were then transferred to a silanized 13  $\times$  100 glass test tube. Three

hundred microliters (300  $\mu$ L) of acetonitrile was then added to the spin column, to wash off all of the permethylated glycan. Spin columns were then centrifuged at 10 000 rpm (5000g) for 30 s to collect the acetonitrile that was pooled with the rest of the sample. To the liquid sample was added 3.5 mL of 0.5 M NaCl, followed by 1.2 mL of chloroform. Liquid/liquid extraction was performed 3 times, saving the chloroform layers, which were dried under a gentle stream of nitrogen.

**Glycan Methylation Analysis.** The following procedure was adapted from Heiss et al.<sup>23</sup> trifluoroacetic acid (TFA) hydrolysis, reduction of sugar aldehydes, acetylation of nascent hydroxyl groups, and then final cleanup.

**Trifluoroacetic Acid (TFA) Hydrolysis.** Three hundred twenty five microliters (325  $\mu$ L) of 2 M TFA was added to each sample, which was then capped tightly and heated at 121  $^{\circ}$ C for 2 h. TFA was then removed by heat-assisted evaporation under a gentle stream of nitrogen.

**Reduction of Sugar Aldehydes.** A fresh 10 mg/mL solution of sodium borohydride in freshly prepared 1 M ammonium hydroxide was prepared and added (475  $\mu$ L) to each test tube, mixed thoroughly, and allowed to react for 1 h at room temperature. Residual borate was removed by adding five drops of methanol to each sample, drying under nitrogen, then adding 125  $\mu$ L of 9:1 (v/v) methanol (MeOH):acetic acid and drying again under nitrogen. Samples were then dried for  $\sim$ 30 min in a vacuum desiccator before proceeding.

**Acetylation of Nascent Hydroxyl Groups.** Two hundred and fifty microliters (250  $\mu$ L) of freshly made water-saturated acetic anhydride (16:234 (v/v) water:acetic anhydride) was added to each sample, which was mixed thoroughly to dissolve as much of the sample residue as possible. Next, 230  $\mu$ L of concentrated TFA was added to each sample, which was then mixed, capped, and incubated at 50  $^{\circ}$ C for 10 min.

**Final Cleanup.** Two milliliters (2 mL) of dichloromethane was added to each sample, along with 2 mL of water. Liquid/liquid extraction carried out twice with water. The final organic layer was then dried in a silanized autosampler vial under nitrogen and reconstituted in eight drops of acetone, mixed, capped, and placed on the GC-MS autosampler rack.

Overall sample throughput is limited by the time required for sample preparation. One analyst can reasonably process  $\sim$ 60–75 samples per week. We anticipate that automated sample processing robotics will be able to significantly reduce this bottleneck in throughput.

**Gas Chromatography–Mass Spectrometry.** GC/MS was carried out on an Agilent Model A7890 gas chromatograph (equipped with a CTC PAL autosampler) coupled to a Waters GCT (time-of-flight) mass spectrometer.

One microliter (1  $\mu$ L) was injected in split mode onto an Agilent split-mode liner (Cat. No. 5183-4647) containing a small plug of silanized glass wool, maintained at 280  $^{\circ}$ C. All injections were made in duplicate: once at a split ratio of 50 and once at a split ratio of 75. Using helium as the carrier gas (0.8 mL/min, constant flow mode), samples were analyzed via chromatography over a 30-m DB-5 ms GC column. The oven was initially held at 165  $^{\circ}$ C for 0.5 min, followed by ramping at 10  $^{\circ}$ C/min to 265  $^{\circ}$ C then immediately ramping at 30  $^{\circ}$ C/min to 325  $^{\circ}$ C and holding for 3 min (15.5 min of total run time). The transfer line was maintained at 250  $^{\circ}$ C. Sample components eluting from the GC column were subjected to electron ionization (70 eV, 250  $^{\circ}$ C) and analyzed from  $m/z$  40 to  $m/z$  800 with a “scan cycle” time of 0.2 s. The mass

spectrometer was tuned and calibrated (to within 10 ppm mass accuracy) daily, using perfluorotributylamine.

**Data Analysis.** Initial identification of PMAAs was made through the analysis of glycan standards and verified through comparison with the online electron ionization mass spectral library of PMAAs at the University of Georgia's Complex Carbohydrate Research Center: <http://www.ccrcc.uga.edu/databases/index.php#>.

The topmost abundant and/or diagnostic fragment ions for each glycan node in blood plasma/serum were summed (using a 0.15 Da extracted ion chromatogram mass window) for quantification (see Table S1 in the Supporting Information). Quantification was carried out by integration of summed extracted ion chromatogram peak areas in automated fashion, using QuanLynx software. Integrated peaks were manually verified then exported to a spreadsheet for further calculation.

All statistical analyses, including the generation of receiver operating characteristic (ROC) curves, were carried out using XLSTAT Version 2012.3.01. All *t*-tests for significant differences between group means were two-sided and pre-evaluated for variance scedasticity. No weighting was employed during analysis of variance (ANOVA) or ROC calculations.

## RESULTS AND DISCUSSION

**Strategy and Initial Development.** For decades now, glycan methylation analysis (Figure 2) has been employed to collect monosaccharide-specific linkage information from preisolated glycans. Given the fact that numerous monosaccharide-specific linkage patterns (i.e., glycan nodes) are created by one or just a few GTs (see Table S2 in the Supporting Information), our goal was to enable glycan methylation analysis as a biomarker development tool by adapting it for routine use with common human biological specimens—minimizing or eliminating sample prefractionation steps.

Solid-phase sodium hydroxide-based permethylation procedures were first developed by Cicanu and co-workers<sup>24–26</sup> and were later refined into online and spin-column based approaches by Kang et al.<sup>27,28</sup> A spin-column based procedure reported in 2009 by Goetz, Novotny, and Mechref<sup>22</sup> discussed the specific chemical release of O-glycans from intact proteins and, for us, represented a promising front-end preparatory step. With little modification, we found that this method could not only release O-linked protein glycans but also, when coupled with a TFA-based methylation analysis protocol,<sup>23</sup> resulted in the release and detection of partially methylated alditol acetates (PMAAs) from N-linked protein glycans as well as glycolipids (Figure 3). As expected, all forms of hexose (plus xylose) and N-acetylhexosamine (HexNAc) residues were detectable. Sulfated, hexuronic, and sialic acid residues were only detected *indirectly*, vis-à-vis their linkage positions. Reducing-end monosaccharides in N-linked glycans appeared in the final analysis, unaffected by their unique N-atom linkage. This was evidenced by the routine detection of the PMAA corresponding to 4,6-linked GlcNAc (4,6-GlcNAc) in blood plasma samples (see Figure 1). Based on the database research conducted to create Table S2 in the Supporting Information, there is only one GT capable of producing this glycan node— $\alpha$ -(1,6)-fucosyltransferase—which exclusively catalyzes the addition of a fucose residue to the 6-position of the reducing-end 4-linked GlcNAc residue in N-glycans.

The suitability of this approach for direct application with 10- $\mu$ L volumes of whole biofluids and homogenized tissue samples

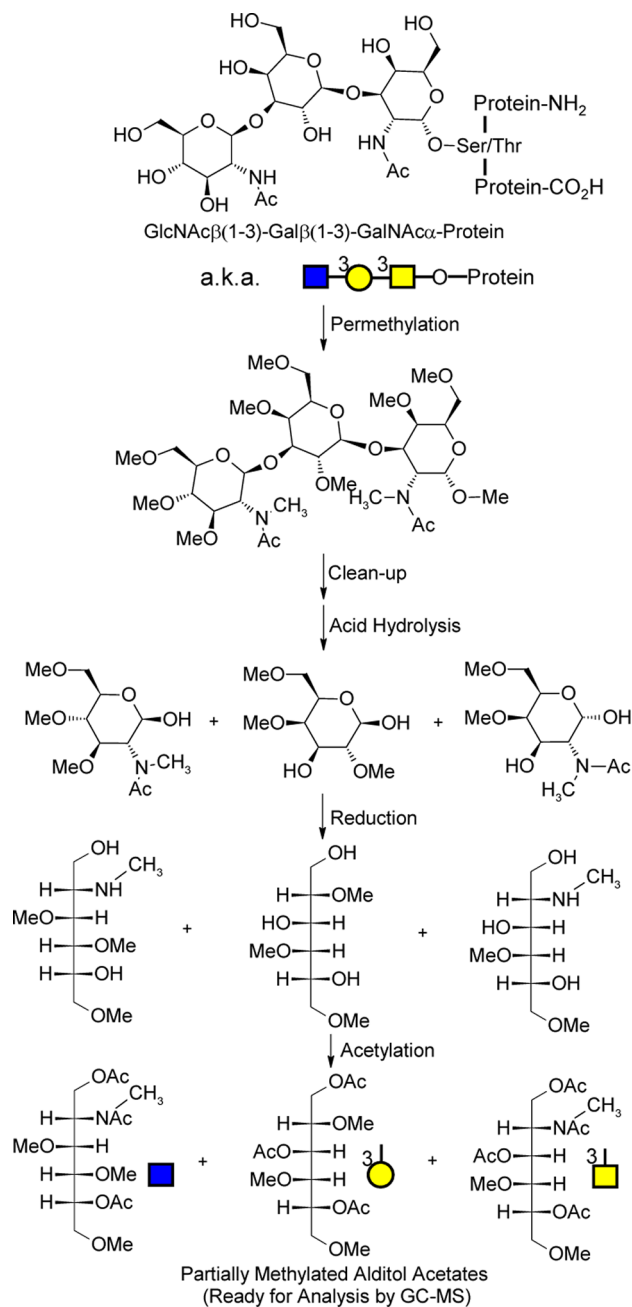


**Figure 2.** Molecular overview of the global glycan methylation analysis procedure. An O-linked glycan is illustrated; these are released during the permethylation process, which has been adapted from Goetz.<sup>22</sup> Following permethylation and hydrolysis, monosaccharides are reduced and nascent hydroxyl groups “marked” by acetylation. The unique pattern of methylation and acetylation in the final partially methylated alditol acetates (PMAAs) corresponds to the unique “glycan node” in the original intact polymer and provides the molecular basis for separation and quantification by GC-MS. N-linked and glycolipid glycans are released as linkage-marked monosaccharides during acid hydrolysis.

was assessed and, in every biomatrix tested to date, proved qualitatively compatible (see Figures 1 and 4). These biomatrix compatibility findings opened up the technique to a wide variety of potential clinical applications. In practical terms, however, blood plasma represented the most readily available biomatrix for assessing the potential clinical utility of the technology.

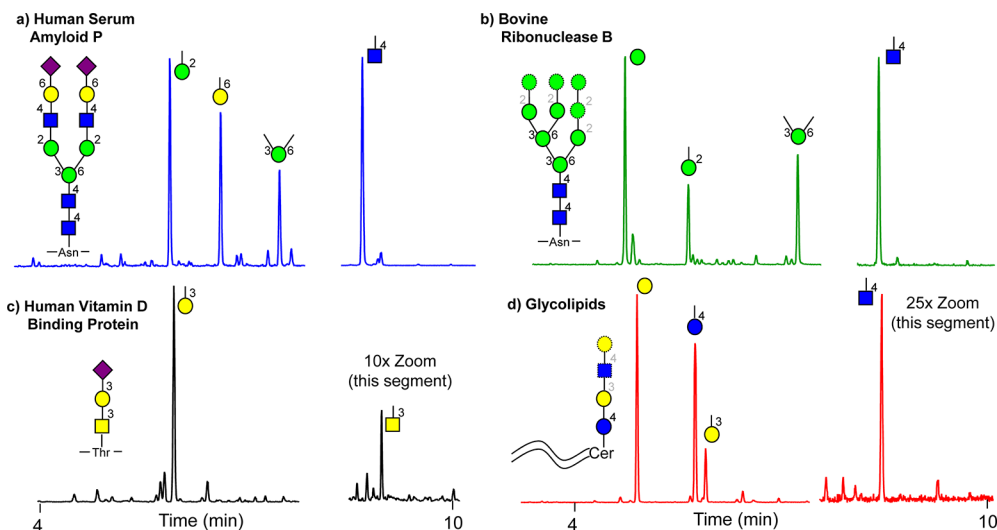


**Figure 3.** Evidence that N-linked and glycolipid glycans were captured by the cleanup protocol and subsequently subjected to methylation analysis. This occurred despite the fact that they were not released during permethylation, like O-linked glycans:<sup>22</sup> (a) prepurified Human Serum Amyloid P (contains only one complex-type N-linked glycan<sup>46,47</sup>), (b) prepurified Bovine Ribonuclease B (RNase B, contains only one high mannose N-linked glycan<sup>48,49</sup>), (c) prepurified Human Vitamin D Binding Protein (DBP, containing a NeuNAc2–3Gal1–3GalNAc O-linked glycan and no N-linked glycans<sup>50,51</sup>), and (d) prepurified neutral glycosphingolipids from human granulocytes (largely characterized by their lactose (Gal1–4Glc)-base-, 3-Gal-, and 4-GlcNAc-containing structures). The extracted-ion chromatograms and symbol legend in this figure are the same as those in Figure 1. Dotted borders around monosaccharides and greyed out linkage numbers indicate potential heterogeneity in the glycan structure across different protein or lipid molecules.

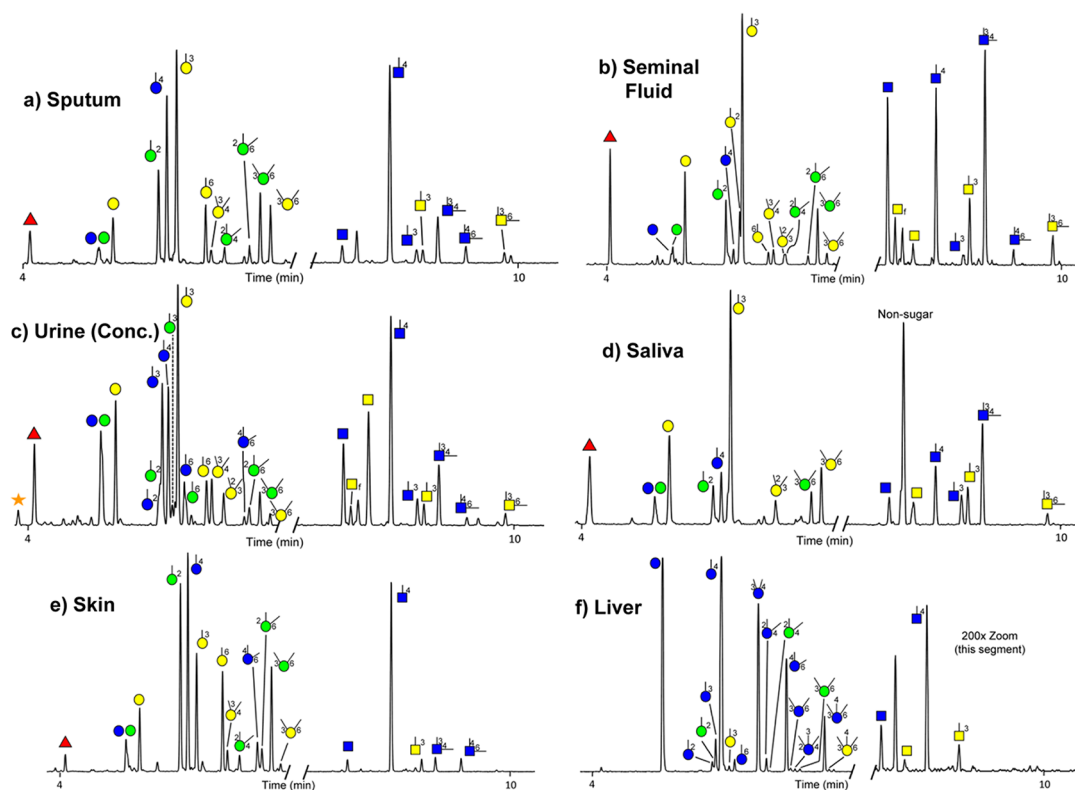


**Figure 4.** Illustrative results from biomatrix compatibility studies. The analytical technique may be applied to 10- $\mu$ L volumes of any whole biofluid or homogenized tissue. Qualitatively diverse results are obtained for (a) sputum (homogenized), (b) seminal fluid (without sperm), (c) urine (concentrated  $\sim 10\times$  prior to analysis), (d) saliva, (e) skin harvested from an abrasion wound, and (f) liver (bovine). The figure legend is the same as that provided in Figure 1. The symbol “f” next to terminal t-GalNAc in the urine sample indicates a furanose (5-membered) ring structure, which likely arises from the presence of some structurally interchangeable free GalNAc in the sample. Glycan nodes derived from glycogen dominate the liver sample.

**Evaluation in Lung Cancer.** Following an initial evaluation of reproducibility in blood plasma (described below), we

applied the new analytical technology to a cross-sectional pilot study of 59 archived blood plasma samples from patients

enrolled in the Lung Cancer in Central and Eastern Europe (CEE) study.<sup>29</sup> Summary information on gender, age, and smoking history is shown in Table 1. Additional detailed

**Table 1. Summary Clinical Information on Gender, Age, and Smoking Status for the 59 Samples Analyzed from the Lung Cancer in Central and Eastern Europe (CEE) Study**

|                   | gender             | age <sup>a</sup> | tobacco pack years <sup>b</sup> |
|-------------------|--------------------|------------------|---------------------------------|
| controls          | 15 male, 14 female | 63.1 ± 7.6       | 17.3 ± 15.2                     |
| lung cancer cases | 16 male, 14 female | 60 ± 10.7        | 27.0 ± 20.7                     |

<sup>a</sup>Student's *t*-test *p*-value for controls versus cases = 0.21. <sup>b</sup>Student's *t* test *p*-value for controls vs cases = 0.046.

information on the patients enrolled in this study can be found online (see Tables S3 and S4 in the Supporting Information). In most cases, samples from lung cancer patients were taken within a few days of initial diagnosis. Controls in this study were matched to the lung cancer patients by age, gender, and smoking status and were enrolled upon visiting participating clinics for non-neoplastic conditions unrelated to tobacco smoking.

Randomized samples were analyzed blind in six separate batches. Despite the addition of heavy, stable-isotope labeled monosaccharides to each sample as internal standards, we found that, generally, the ratios of endogenous glycan nodes to each other (GNRs) tended to provide greater analytical precision than the ratios of individual glycan nodes to stable-

isotope labeled internal standards (iGNs) (see Table 2 and Table S5 in the Supporting Information, which are described in additional detail below). In the CEE group of samples, 8 iGNs and 29 GNRs were found to be significantly different ( $p < 0.005$ ) in the lung cancer cases, versus controls. The top 2 performing GNRs had ROC *c*-statistics in the range of 0.8–0.9 (see Figure 5). The top 12 performing GNRs had ROC *c*-statistics of >0.75, which was better than any single iGN (see Table 2 and Table S5 in the Supporting Information).

To evaluate if these GNRs might be mere indicators of smoking status, the ROC curve analysis was repeated for smokers only and on the basis of smokers (including current and former) versus nonsmokers (i.e., never-smokers/no smoking history), regardless of cancer status (see Table 2). ROC curve analysis for smokers-only demonstrated negligible differences, compared to when nonsmokers were included in the analysis (Table 2). ROC curve analysis for smokers versus nonsmokers (regardless of cancer status) demonstrated an across-the-board loss of diagnostic power for 10 of the top 12 GNRs (see Table 2)—indicating that these markers are linked to the presence of cancer and not smoking history. Interestingly, the two GNR ROC *c*-statistics that remained the same or increased in this comparison had the same common denominator (3-GalNAc). The biological relationship of this glycan node to smoking, if any, is not yet clear.

**Analytical Validation in Blood Plasma.** Analytical validation of the approach in blood plasma was undertaken with the goals of determining reproducibility (intraday and interday precision), sample stability, consistency of results in

**Table 2. Analytical Reproducibility and Clinical Performance Characteristics of the 12 Top-Performing Blood Plasma-Based Glycan Node Ratios (GNRs) in Lung Cancer<sup>a</sup>**

| glycan node ratio, GNR | intra-assay precision (%) CV | inter-assay precision (%) CV | ROC AUC ± SE  |  |   | ROC AUC ± SE  |
|------------------------|------------------------------|------------------------------|---|--|---|---|
|                        |                              |                              | cancer ( <i>n</i> = 28) vs noncancer ( <i>n</i> = 29) | smokers only: cancer ( <i>n</i> = 25) vs nonsmokers ( <i>n</i> = 23) | trend in cancers (increased (I) or decreased (D)) | smokers ( <i>n</i> = 48) vs nonsmokers ( <i>n</i> = 9) <sup>b</sup> |
| t-Gal/6-Gal            | 2.34                         | 3.76                         | 0.878 ± 0.051 <sup>c</sup>                            | 0.897 ± 0.048 <sup>c</sup>   | D   | 0.681 ± 0.087 <sup>d</sup>  |
| t-Gal/3,6-Man          | 4.35                         | 5.69                         | 0.869 ± 0.048 <sup>c</sup>                            | 0.868 ± 0.051 <sup>c</sup>   | D   | NS  |
| 2,4-Man/3-GalNAc       | 7.76                         | 11.97                        | 0.793 ± 0.055   | 0.775 ± 0.062  | I   | 0.804 ± 0.057   |
| t-Gal/2,4-Man          | 7.06                         | 7.38                         | 0.79 ± 0.06   | 0.789 ± 0.063  | D   | NS  |
| 2,4-Man/3,4,6-Man      | 8.59                         | 11.13                        | 0.786 ± 0.06  | 0.775 ± 0.066  | I   | NS  |
| 2-Man/2,4-Man          | 6.08                         | 8.93                         | 0.78 ± 0.058  | 0.781 ± 0.062  | D   | NS  |
| 6-Gal/3-GalNAc         | 5.29                         | 9.56                         | 0.777 ± 0.058   | 0.778 ± 0.064  | I   | 0.88 ± 0.043  |
| 2,4-Man/t-GlcNAc       | 4.47                         | 5.12                         | 0.772 ± 0.058   | 0.776 ± 0.062  | I   | NS  |
| 6-Gal/3,4,6-Man        | 4.61                         | 7.15                         | 0.772 ± 0.06  | 0.767 ± 0.065  | I   | NS  |
| 2,6-Man/3,4,6-Man      | 5.24                         | 5.59                         | 0.766 ± 0.063   | 0.749 ± 0.069  | I   | NS  |
| 3,6-Man/3,4,6-Man      | 3.35                         | 4.89                         | 0.764 ± 0.061   | 0.752 ± 0.066  | I   | NS  |
| t-Gal/2,6-Man          | 5.9                          | 9.82                         | 0.76 ± 0.064  | 0.767 ± 0.067  | D   | NS  |

<sup>a</sup>Reproducibility was assessed through the analysis of six samples per batch on three separate days. Diagnostic capacity was maintained in the analysis of smokers only and, with the exception of two node ratios that share a common denominator (3-GalNAc), there was a loss of diagnostic capacity for smokers vs. non-smokers. <sup>b</sup>Regardless of cancer status. NS = not statistically significant from an ROC AUC of 0.5. <sup>c</sup>Including two lung cancer-group outliers that lie on the *opposite side* of the control distribution and are *completely separate* from it gives ROC *c*-statistics (AUCs) of 0.82 ± 0.062 and 0.81 ± 0.060 for the top two node ratios, respectively (0.83 ± 0.063 and 0.80 ± 0.064 for the smokers only group). <sup>d</sup>The difference between the “cancer vs. noncancer” group is 0.197 ± 0.10 (statistically significant at the 2σ-level).

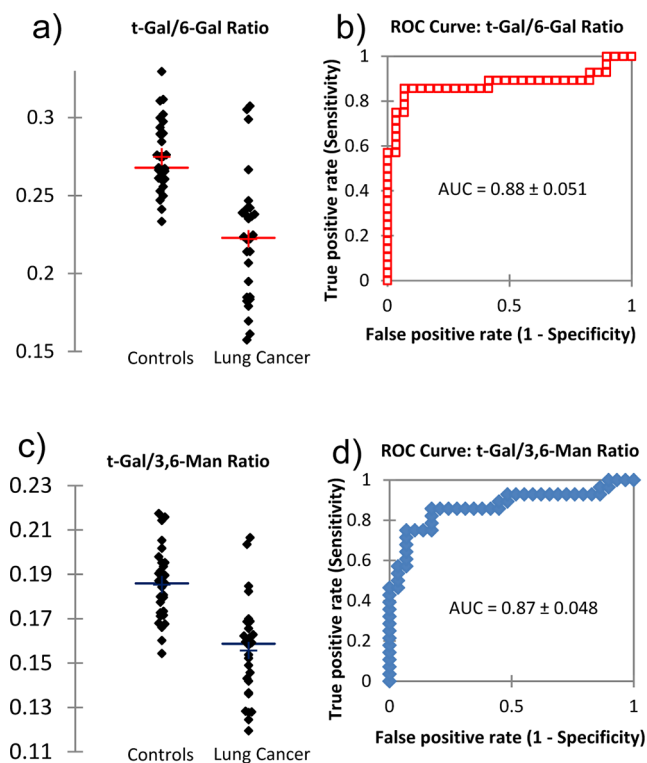


**Figure 5.** Clinical performance of the top blood plasma-based glycan node ratios (GNRs) in distinguishing newly diagnosed lung cancer patients ( $n = 28$ ) from age/gender/smoking status-matched controls ( $n = 29$ ): (a) univariate distribution of the t-Gal/6-Gal GNR, (b) ROC curve for t-Gal/6-Gal, (c) univariate distribution of the t-Gal/3,6-Man GNR, and (d) ROC curve for t-Gal/3,6-Man. For both of these GNRs, the same two samples from squamous cell carcinoma patients produced two outliers on the opposite side of the control distribution. Since they were completely separate from the control distribution, they were excluded from the ROC curve analysis. Table 1 summarizes the clinical performance characteristics for the top 12 diagnostic GNRs in lung cancer.

serum and four different types of plasma, autosampler stability, and analytical sensitivity and linearity of response. Because of space constraints and the need to avoid the presentation of copious amounts of superfluous data, the analytical validation parameters described below are largely contextualized to the top 12 performing GNRs in lung cancer (see Table 2).

**Precision/Reproducibility.** Despite the addition of heavy, stable-isotope labeled monosaccharides to each plasma sample as internal standards, we found that, based on the analysis of six aliquots of the same plasma sample per day on three different days, the ratios of individual glycan nodes to stable-isotope labeled internal standards (iGNs) were not highly reproducible (see Table S5 in the Supporting Information) and that the ratios of endogenous glycan nodes to each other (GNRs) tended to provide greater analytical precision. Since  $\sim 20$  iGNs were routinely detected in plasma samples, this meant that over 200 GNRs were available for assessment of reproducibility. Of these GNRs, over 80 had both intra-assay and inter-assay reproducibility of  $<15\%$ . The analytical precision of the top 12 performing GNRs in lung cancer are reported in Table 2.

**Sample Stability.** GNR stability in blood plasma samples was assessed by creating 12 aliquots of a single sample then placing 6 back into the  $-80\text{ }^{\circ}\text{C}$  freezer and leaving the remaining 6 at room temperature overnight. None of the top 6,

but 2 of the top 12 lung cancer GNRs demonstrated statistically significant difference between the batches (see Table S6 in the Supporting Information). However, these apparent differences were subtle and may have been due to abnormally tight intra-assay precision as the overall differences between the batches were  $<12\%$ .

**Effect of Blood Collection Type.** Matched sets of blood serum, 3.8% sodium citrate,  $\text{Na}_2\text{EDTA}$ ,  $\text{K}_2\text{EDTA}$ , and  $\text{K}_3\text{EDTA}$  plasma samples were collected from 22 healthy volunteers. Glycan nodes were then analyzed in the resulting 110 samples. Analysis of the results for the top 12 lung cancer GNRs by Repeated Measures ANOVA followed by the Ryan–Einot–Gabriel–Welsch (REGW) multiple comparison test demonstrated no significant differences between the blood collection types (see Table S7 in the Supporting Information).

**Autosampler Stability.** Autosampler stability was assessed over the time span required to inject 48 samples ( $\sim 14.5\text{ h}$ ), which was the largest batch size employed during the analysis of samples reported in this paper. Four data points from the same sample were acquired three times—at the beginning, middle, and end of this time period. Passing stability was designated to be within 10% of the average of the first two data points. Autosampler stability passed for the top 12 lung cancer GNRs, except the three with HexNAc nodes as the denominator (see Figure S1 in the Supporting Information)—which were of minimal interest since 2 of these 3 appear to be more diagnostic of smoking rather than lung cancer and the third is not in the top 6 GNRs (see Table 2).

**Analytical Sensitivity and Linearity of Response.** IUPAC defines analytical sensitivity as the ability of an analytical procedure to produce a change in signal for a defined change in analyte quantity.<sup>30</sup> They add that, in most cases, this parameter can be observed as the slope of a calibration curve. The fact that strong, statistically significant differences were detected in numerous iGNs and GNRs between the CEE lung cancer cases and controls (see Table 2 and Table S5 in the Supporting Information) suggested that analytical sensitivity was more than adequate to impart the technique with potential clinical applicability—but the expense and limited availability of glycan polymer standards precluded a formal assessment of the analytical sensitivity for all 12 of the top lung cancer GNRs. However, the instrument response ratio of t-Gal/6-Gal versus the actual molar ratio of t-Gal/6-Gal was assessed through the use of *N*-acetyllactosamine (Gal1–4GalNAc) and 6-sialyl-*N*-acetyllactosamine (NeuNAc2–6Gal1–4GalNAc) standards. These were mixed together in ratios spanning the physiologically observed range in blood plasma, such that overall signal intensities approximated those from blood plasma samples. Following analysis on two different days, the resulting data were employed to construct a standard curve (see Figure S2 in the Supporting Information). The standard curve was linear ( $R^2 = 0.993$ ) and had a slope of 1.31, indicating a change of greater than 1:1 in instrument response per change in actual glycan node molar ratio.

**Other Analytical Validation Considerations.** The goal of this study was to evaluate changes in the relative abundance of readily detectable glycan nodes as potential clinical markers; this is a distinct and separate goal from quantifying low-abundance glycan nodes. As such, unlike most conventional assays, raw sensitivity (i.e., limits of detection and limits of quantification) was not a parameter of significant concern because, for each biomatrix, a particular set of glycan nodes was present in every sample at readily detectable levels. For

example, although not visible with the particular extracted-ion chromatograms from plasma shown in Figure 1, there were over 18 individual glycan nodes with signal/noise (S/N) ratios of >10 in every plasma sample of hundreds of individual samples tested to date. Thus, in the absence of a specific need to detect low-abundance glycan node(s), raw detection limits were of little practical importance or value, relative to analytical sensitivity. In the future, if raw detection limits are required for a particular application, they will need to be investigated on a biomatrix-specific basis.

Since this is a technique for the relative quantification of the constituent components of heterogeneous biological polymers, *accuracy* cannot be defined by any single molecular standard. But this does not rule out clinical utility or applicability: To achieve these things without a definition of absolute accuracy, good reproducibility/precision of iGN/GNR measurement will be critical (as documented above), but it will eventually have to be coupled with a mechanism to facilitate interlaboratory transferability—for example, through establishment of a “gold standard” sample that can be shared across laboratories or through instrument-specific calibration with predefined standard curves (such as that in Figure S2 in the Supporting Information). Since the latter will have to be based on particular chemical standards, they still will not be able to define accuracy in an absolute sense and, at best, will only ever be considered to provide results that are *approximately* accurate according to strict definition; however, this is essentially irrelevant when it comes to practical application.

**Disease Specificity.** To further evaluate the specificity of the top-performing blood plasma GNRs for lung cancer, two additional sets of samples were analyzed for comparison. The first set consisted of biobank-purchased serum samples from 80 healthy individuals, an additional 16 lung cancer patients, 10 colorectal cancer and 59 prostate cancer patients. The second set consisted of a cross section of patients from a University of Arizona diabetes study who had undergone an oral glucose tolerance test and ranged from healthy (normal glucose tolerance, NGT,  $n = 18$ ), to pre-diabetic (impaired glucose tolerance, IGT,  $n = 12$ ), to stark Type 2 diabetes (T2D,  $n = 32$ ), to T2D with cardiovascular complications (T2D w/CVD,  $n = 26$ ). Analysis of the top 6 lung cancer GNRs (Table 2) in these samples by ANOVA, followed by the REGW multiple comparison test, demonstrated a general grouping of lung cancer and colorectal cancer separate from the other sample sets, with T2D aligning more closely with lung and colorectal cancer than did prostate cancer (see Figure S3 in the Supporting Information). These cross-disease comparisons suggested that the GNR markers in blood were not just fluctuating with inflammation and possessed at least a limited degree of specificity for certain types of cancer.

Comparison of GNRs in biobank-purchased serum samples from cancer patients with those from nominally healthy individuals revealed general consistency of GNR behavior in the two lung cancer groups (see Table 2 and Table S8 in the Supporting Information). In addition, there was partial GNR profile overlap between lung and colorectal cancer but not prostate cancer (see Table 2 and Tables 8–10 in the Supporting Information). Based on increases in ROC  $c$ -statistics, GNRs were better at distinguishing lung cancer patients from fully healthy individuals than from well-match controls (Table 2 and Table S8 in the Supporting Information), which is an unsurprising but useful observation to note when it comes to the design of biomarker studies. GNRs in serum did

not appear to be particularly diagnostic in prostate cancer (see Table S10 in the Supporting Information).

**Biological Implications.** Glycan nodes observed via this technique are necessarily derived from the most abundant glycan source in the sample under consideration. In blood plasma, roughly half of the glycoproteins are immunoglobulins/complement protein and the other half are liver glycoproteins. Unless near-milligram-per-milliliter plasma concentrations are reached, cancer glycoprotein shedding is unlikely to contribute more than an unobservable fraction to the total plasma glycoprotein content. This means that cancer-induced alterations to the humoral immune system and/or the liver are most likely responsible for the alterations in plasma glycan nodes observed here. Although the mechanisms behind such phenomena (e.g., those discovered by Narisada et al.<sup>31</sup> and Kitazume et al.<sup>32</sup>) are varied and the phenomena themselves are only partially understood, they are by no means unknown,<sup>2–18</sup> even in non-neoplastic diseases.<sup>19,20</sup>

Glycan source notwithstanding, aberrant activity of at least two different GTs in lung and colorectal cancer patients was detected (see Table 2 and Tables S5 and S8–S10 in the Supporting Information). A table of GTs responsible for producing the glycan nodes observed in humans is provided online (see Table S2 in the Supporting Information):

- (1) ST6Gal-I: Six (6) of the top 12-performing GNRs in lung cancer (see Table 2) and 5 of the top 7 GNRs in colorectal cancer (Table S9 in the Supporting Information) involved t-Gal and/or 6-Gal. When their behavior was considered in cancer cases, compared to controls, these GNRs showed fluctuations that were consistent with minor changes in t-Gal ( $p = 0.04$ ) and significant increases in 6-Gal ( $p = 8.6 \times 10^{-4}$ ; ROC  $c$ -statistic =  $0.737 \pm 0.064$  (see Table S5 in the Supporting Information)). Together, these data indicated increased  $\beta$ -galactoside: $\alpha$ -2,6-sialyltransferase (ST6Gal-I) enzyme activity—a phenomenon for which there is evidence in cancer cells from numerous other carcinomas including those of the colon/rectum,<sup>33,34</sup> breast,<sup>35</sup> brain (non-neuroectodermal epithelial-like tumors),<sup>36</sup> cervix,<sup>37</sup> and liver (transgenic mouse model of hepatocellular carcinoma),<sup>38</sup> as well as in choriocarcinoma (cell lines)<sup>39</sup> and acute myeloid leukemia.<sup>40</sup>
- (2) GnT-IV: Five (5) of the top 12 lung cancer GNRs (see Table 2) and 2 of the top 7 colorectal cancer GNRs (see Table S9 in the Supporting Information) provided evidence for elevated quantities of 2,4-Man. In addition, the 2,4-Man iGN in CEE lung cancer patients was significantly higher than in the controls ( $p = 3.4 \times 10^{-4}$ ; ROC  $c$ -statistic =  $0.747 \pm 0.063$  (see Table S5 in the Supporting Information)). Increased 2,4-Man is mediated through increased UDP-*N*-acetylglucosamine: $\alpha$ -1,3-*D*-mannosidase  $\beta$ 1,4-*N*-acetylglucosaminyltransferase IV (GnT-IV) activity. Generally speaking, this enzyme has been documented as overactive during oncogenesis and differentiation.<sup>41</sup> Evidence for its overexpression has been found in cancer cells from colorectal carcinoma,<sup>42</sup> choriocarcinoma,<sup>43</sup> hepatocellular carcinoma,<sup>44</sup> and pancreatic cancer (GnT-IVb form).<sup>45</sup>

To our knowledge this is the first report of altered activity for either ST6Gal-I or GnT-IV in lung cancer patients; in our opinion, the fact that these changes may not be derived directly from tumor cells themselves makes the findings intriguing,



particularly with regard to potential therapeutic implications embedded in the underlying mechanism(s). Based on the CEE group of samples, a total of 12 iGNs were significantly increased in lung cancer patient plasma, providing evidence for activity changes in numerous other GTs as well, including fucosyltransferases (*vis-à-vis*, increased t-Fuc and 3,4-GlcNAc) and GnT-V (*vis-à-vis*, increased 2,6-Man) (see Tables S2 and S5 in the Supporting Information).

Four of the seven increasing GNRs in lung cancer (Table 2) contained 3,4,6-Man as their denominator, providing suggestive evidence for decreased  $\beta$ 1,4-N-acetylglucosaminyltransferase III (GnT-III) activity, which is the GT responsible for adding “bisecting GlcNAc” to N-linked glycans. However, the change in the 3,4,6-Man iGN was not statistically significant. Notably, the 3,6-Man iGN increased in CEE lung cancer patients relative to controls ( $p = 1.4 \times 10^{-3}$ ; see Table S5 in the Supporting Information)—suggesting an overall increase in N-glycans and a relative inability of GnT-III to keep pace.

## CONCLUSIONS

There is an urgent need for blood-borne markers of risk and progression in lung cancer, as well as other types of cancer (and glycan-affective disorders) to which this analytical approach will likely be applicable. Based on current knowledge of human GTs, the glycan nodes 6-Gal, 2,4-Man, 2,6-Man, and 3,4,6-Man represent 1:1 (or nearly 1:1) molecular surrogates for ST6Gal-I, GnT-IV, GnT-V, and GnT-III, respectively—and there are other glycan nodes that hold this same relationship with their respective GTs (Table S2 in the Supporting Information). Additional glycan nodes, such as 3-Gal, may represent the activity of multiple GTs but they are still potentially modulated by the aberrant expression of just one of the GTs that leads to their existence.

By condensing and pooling together, into a single analytical signal, the inherent molecular heterogeneity introduced by aberrantly expressed GTs (Figure 1)—and doing so for multiple GTs simultaneously from 10  $\mu$ L of whole, unprocessed biofluid without the use of enzyme or antibody reagents—this analytical approach represents a promising means by which to access glycans as disease markers. Its utility is expected to improve further, once it can be applied to hundreds of well-characterized patient samples for which outcome information is available, then coupled to multivariate modeling algorithms to create disease-specific prognostic biosignatures. Finally, we note that cancer-induced aberrant glycans in plasma/serum may be diluted by significant quantities of normal glycans; as such, going forward, we feel that application of this technology to biofluids or tissues obtained directly from putatively cancerous organs (e.g., as demonstrated in Figure 4) may represent a more powerful use of this technology to address specific medical needs for better cancer markers.

## ASSOCIATED CONTENT

### Supporting Information

This material is available free of charge via the Internet at <http://pubs.acs.org>.

## AUTHOR INFORMATION

### Corresponding Author

\*Tel.: 480-727-9928. Fax: 480-727-9464. E-mail: [chad.borges@asu.edu](mailto:chad.borges@asu.edu)

## Notes

The authors declare no competing financial interest.

## ACKNOWLEDGMENTS

This research was supported by a Flinn Foundation Award and, in part, by NIH Grant Nos. R01DK082542 and R24DK083948, as well as Grant No. GM62116 to the Consortium for Functional Glycomics. We thank Dr. Mark Holl and Dr. Mia Hashibe for helpful discussions. We also thank the national PIs of the CEE study for allowing the use of the samples: Drs. D. Zaridze, Moscow, Russia; J. Lissowska, Warsaw, Poland; N. Szeszenia-Dabrowska, Lodz, Poland; E. Fabianova, Banska-Bystrica, Slovakia; P. Rudnai, Budapest, Hungary; D. Mates, Bucharest, Romania; V. Bencko, Prague, Czech Republic; L. Foretova, Brno, Czech Republic; V. Janout, Olomouc, Czech Republic.

## REFERENCES

- (1) Varki, A.; Kannagi, R.; Toole, B. P. In *Essentials of Glycobiology*, 2nd Edition; Varki, A., Cummings, R. D., Esko, J. D., Freeze, H. H., Stanley, P., Bertozzi, C. R., Hart, G. W., Etzler, M. E., Eds.; Cold Spring Harbor Laboratory Press: Cold Spring Harbor, NY, 2009; Chapter 44.
- (2) Gercel-Taylor, C.; Bazzett, L. B.; Taylor, D. D. *Gynecol. Oncol.* **2001**, *81*, 71–76 (DOI: 10.1006/gyno.2000.6102).
- (3) An, H. J.; Miyamoto, S.; Lancaster, K. S.; Kirmiz, C.; Li, B.; Lam, K. S.; Leiserowitz, G. S.; Lebrilla, C. B. *J. Proteome Res.* **2006**, *5*, 1626–1635 (DOI: 10.1021/pr060010k).
- (4) Kanoh, Y.; Mashiko, T.; Danbara, M.; Takayama, Y.; Ohtani, S.; Egawa, S.; Baba, S.; Akahoshi, T. *Anticancer Res.* **2004**, *24*, 3135–3139.
- (5) Kyselova, Z.; Mechref, Y.; Al Bataineh, M. M.; Dobrolecki, L. E.; Hickey, R. J.; Vinson, J.; Sweeney, C. J.; Novotny, M. V. *J. Proteome Res.* **2007**, *6*, 1822–1832 (DOI: 10.1021/Pr060664t).
- (6) Okuyama, N.; Ide, Y.; Nakano, M.; Nakagawa, T.; Yamanaka, K.; Moriwaki, K.; Murata, K.; Ohigashi, H.; Yokoyama, S.; Eguchi, H.; Ishikawa, O.; Ito, T.; Kato, M.; Kasahara, A.; Kawano, S.; Gu, J.; Taniguchi, N.; Miyoshi, E. *Int. J. Cancer* **2006**, *118*, 2803–2808 (DOI: 10.1002/ijc.21728).
- (7) Zhao, J.; Patwa, T. H.; Qiu, W.; Shedden, K.; Hinderer, R.; Misk, D. E.; Anderson, M. A.; Simeone, D. M.; Lubman, D. M. *J. Proteome Res.* **2007**, *6*, 1864–1874 (DOI: 10.1021/pr070062p).
- (8) Comunale, M. A.; Lowman, M.; Long, R. E.; Krakover, J.; Philip, R.; Seeholzer, S.; Evans, A. A.; Hann, H. W.; Block, T. M.; Mehta, A. S. *J. Proteome Res.* **2006**, *5*, 308–315 (DOI: 10.1021/pr050328x).
- (9) Goldman, R.; Ransom, H. W.; Varghese, R. S.; Goldman, L.; Bascug, G.; Loffredo, C. A.; Abdel-Hamid, M.; Gouda, I.; Ezzat, S.; Kyselova, Z.; Mechref, Y.; Novotny, M. V. *Clin. Cancer Res.* **2009**, *15*, 1808–1813 (DOI: 10.1158/1078-0432.Ccr-07-5261).
- (10) Aurer, I.; Lauc, G.; Dumic, J.; Rendic, D.; Maticic, D.; Milos, M.; Heffer-Lauc, M.; Flogel, M.; Labar, B. *Coll. Antropol.* **2007**, *31*, 247–251.
- (11) Abd Hamid, U. M.; Royle, L.; Saldova, R.; Radcliffe, C. M.; Harvey, D. J.; Storr, S. J.; Pardo, M.; Antrobus, R.; Chapman, C. J.; Zitzmann, N.; Robertson, J. F.; Dwek, R. A.; Rudd, P. M. *Glycobiology* **2008**, *18*, 1105–1118 (DOI: 10.1093/glycob/cwn095).
- (12) Kyselova, Z.; Mechref, Y.; Kang, P.; Goetz, J. A.; Dobrolecki, L. E.; Sledge, G. W.; Schnaper, L.; Hickey, R. J.; Malkas, L. H.; Novotny, M. V. *Clin. Chem.* **2008**, *54*, 1166–1175 (DOI: 10.1373/clinchem.2007.087148).
- (13) Hongsachart, P.; Huang-Liu, R.; Sinchaikul, S.; Pan, F. M.; Phutrakul, S.; Chuang, Y. M.; Yu, C. J.; Chen, S. T. *Electrophoresis* **2009**, *30*, 1206–1220 (DOI: 10.1002/elps.200800405).
- (14) Arnold, J. N.; Saldova, R.; Galligan, M. C.; Murphy, T. B.; Mimura-Kimura, Y.; Telford, J. E.; Godwin, A. K.; Rudd, P. M. *J. Proteome Res.* **2011**, *10*, 1755–1764 (DOI: 10.1021/pr101034t).

- (15) Bones, J.; Mittermayr, S.; O'Donoghue, N.; Guttman, A.; Rudd, P. M. *Anal. Chem.* **2010**, *82*, 10208–10215 (DOI: 10.1021/ac102860w).
- (16) Kodar, K.; Stadlmann, J.; Klaamas, K.; Sergeev, B.; Kurtenkov, O. *Glycoconjugate J.* **2012**, *29*, 57–66 (DOI: 10.1007/s10719-011-9364-z).
- (17) Chen, G.; Wang, Y.; Qiu, L.; Qin, X.; Liu, H.; Wang, X.; Wang, Y.; Song, G.; Li, F.; Guo, Y.; Li, F.; Guo, S.; Li, Z. *J. Proteomics* **2012**, *75*, 2824–2834 (DOI: 10.1016/j.jprot.2012.02.001).
- (18) Takeda, Y.; Shinzaki, S.; Okudo, K.; Moriwaki, K.; Murata, K.; Miyoshi, E. *Cancer* **2012**, *118*, 3036–3043 (DOI: 10.1002/cncr.26490).
- (19) Parekh, R. B.; Dwek, R. A.; Sutton, B. J.; Fernandes, D. L.; Leung, A.; Stanworth, D.; Rademacher, T. W.; Mizuochi, T.; Taniguchi, T.; Matsuta, K.; et al. *Nature* **1985**, *316*, 452–457.
- (20) Mehta, A. S.; Long, R. E.; Comunale, M. A.; Wang, M.; Rodemich, L.; Krakover, J.; Philip, R.; Marrero, J. A.; Dwek, R. A.; Block, T. M. *J. Virol.* **2008**, *82*, 1259–1270 (DOI: 10.1128/JVI.01600-07).
- (21) Rini, J.; Esko, J.; Varki, A. In *Essentials of Glycobiology*, 2nd Edition; Varki, A., Cummings, R. D., Esko, J. D., Freeze, H. H., Stanley, P., Bertozzi, C. R., Hart, G. W., Etzler, M. E., Eds.; Cold Spring Harbor Laboratory Press: Cold Spring Harbor, NY, 2009; Chapter 5.
- (22) Goetz, J. A.; Novotny, M. V.; Mechref, Y. *Anal. Chem.* **2009**, *81*, 9546–9552.
- (23) Heiss, C.; Klutts, J. S.; Wang, Z.; Doering, T. L.; Azadi, P. *Carbohydr. Res.* **2009**, *344*, 915–920 (DOI: 10.1016/j.carres.2009.03.003).
- (24) Ciucanu, I.; Kerek, F. *Carbohydr. Res.* **1984**, *131*, 209–217.
- (25) Ciucanu, I.; Costello, C. E. *J. Am. Chem. Soc.* **2003**, *125*, 16213–16219 (DOI: 10.1021/Ja035660t).
- (26) Ciucanu, I.; Caprita, R. *Anal. Chim. Acta* **2007**, *585*, 81–85.
- (27) Kang, P.; Mechref, Y.; Klouckova, L.; Novotny, M. V. *Rapid Commun. Mass Spectrom.* **2005**, *19*, 3421–3428 (DOI: 10.1002/Rcm.2210).
- (28) Kang, P.; Mechref, Y.; Novotny, M. V. *Rapid Commun. Mass Spectrom.* **2008**, *22*, 721–734 (DOI: 10.1002/Rcm.3395).
- (29) Brennan, P.; Crispo, A.; Zaridze, D.; Szeszenia-Dabrowska, N.; Rudnai, P.; Lissowska, J.; Fabianova, E.; Mates, D.; Bencko, V.; Foretova, L.; Janout, V.; Fletcher, T.; Boffetta, P. *Am. J. Epidemiol.* **2006**, *164*, 1233–1241 (DOI: 10.1093/aje/kwj340).
- (30) McNaught, A. D.; Wilkinson, A. *IUPAC. Compendium of Chemical Terminology*, 2nd Edition (the “Gold Book”); Blackwell Scientific Publications: Oxford, U.K., 1997. (XML on-line corrected version: <http://goldbook.iupac.org> (2006). Created by M. Nic, J. Jirat, B. Kosata; updates compiled by A. Jenkins. DOI: 10.1351/goldbook; Version: 2.3.2. Last update: Aug. 19, 2012.)
- (31) Narisada, M.; Kawamoto, S.; Kuwamoto, K.; Moriwaki, K.; Nakagawa, T.; Matsumoto, H.; Asahi, M.; Koyama, N.; Miyoshi, E. *Biochem. Biophys. Res. Commun.* **2008**, *377*, 792–796 (DOI: 10.1016/j.bbrc.2008.10.061).
- (32) Kitazume, S.; Oka, R.; Ogawa, K.; Futakawa, S.; Hagiwara, Y.; Takikawa, H.; Kato, M.; Kasahara, A.; Miyoshi, E.; Taniguchi, N.; Hashimoto, Y. *Glycobiology* **2009**, *19*, 479–487 (DOI: 10.1093/glycob/cwp003).
- (33) Vierbuchen, M. J.; Fruechtlich, W.; Brackrock, S.; Krause, K. T.; Zienkiewicz, T. *J. Cancer* **1995**, *76*, 727–735.
- (34) Dall'Olio, F.; Malagolini, N.; di Stefano, G.; Minni, F.; Marrano, D.; Serafini-Cessi, F. *Int. J. Cancer* **1989**, *44*, 434–439.
- (35) Recchi, M. A.; Hebbbar, M.; Hornez, L.; Harduin-Lepers, A.; Peyrat, J. P.; Delannoy, P. *Cancer Res.* **1998**, *58*, 4066–4070.
- (36) Kaneko, Y.; Yamamoto, H.; Kersey, D. S.; Colley, K. J.; Leestma, J. E.; Moskal, J. R. *Acta Neuropathol.* **1996**, *91*, 284–292.
- (37) Wang, P. H.; Li, Y. F.; Juang, C. M.; Lee, Y. R.; Chao, H. T.; Tsai, Y. C.; Yuan, C. C. *Gynecol. Oncol.* **2001**, *83*, 121–127 (DOI: 10.1006/gyno.2001.6358).
- (38) Pousset, D.; Piller, V.; Bureaud, N.; Monsigny, M.; Piller, F. *Cancer Res.* **1997**, *57*, 4249–4256.
- (39) Fukushima, K.; Hara-Kuge, S.; Seko, A.; Ikehara, Y.; Yamashita, K. *Cancer Res.* **1998**, *58*, 4301–4306.
- (40) Skacel, P. O.; Edwards, A. J.; Harrison, C. T.; Watkins, W. M. *Blood* **1991**, *78*, 1452–1460.
- (41) Taniguchi, N.; Korekane, H. *BMB Rep.* **2011**, *44*, 772–781.
- (42) D'Arrigo, A.; Belluco, C.; Ambrosi, A.; Digito, M.; Esposito, G.; Bertola, A.; Fabris, M.; Nofrate, V.; Mammano, E.; Leon, A.; Nitti, D.; Lise, M. *Int. J. Cancer* **2005**, *115*, 256–262 (DOI: 10.1002/ijc.20883).
- (43) Endo, T.; Nishimura, R.; Kawano, T.; Mochizuki, M.; Kobata, A. *Cancer Res.* **1987**, *47*, 5242–5245.
- (44) Yamashita, K.; Totani, K.; Iwaki, Y.; Takamisawa, I.; Tateishi, N.; Higashi, T.; Sakamoto, Y.; Kobata, A. *J. Biochem.* **1989**, *105*, 728–735.
- (45) Ide, Y.; Miyoshi, E.; Nakagawa, T.; Gu, J.; Tanemura, M.; Nishida, T.; Ito, T.; Yamamoto, H.; Kozutsumi, Y.; Taniguchi, N. *Biochem. Biophys. Res. Commun.* **2006**, *341*, 478–482 (DOI: 10.1016/j.bbrc.2005.12.208).
- (46) Tennent, G. A.; Pepys, M. B. *Biochem. Soc. Trans.* **1994**, *22*, 74–79.
- (47) Kiernan, U. A.; Nedelkov, D.; Tubbs, K. A.; Niederkofler, E. E.; Nelson, R. W. *Proteomics* **2004**, *4*, 1825–1829.
- (48) Uniprot Consortium. *Nucleic Acids Res.* **2012**, *40*, D71–D75 (DOI: 10.1093/Nar/Gkr981).
- (49) Prien, J. M.; Ashline, D. J.; Lapadula, A. J.; Zhang, H.; Reinhold, V. N. *J. Am. Soc. Mass Spectrom.* **2009**, *20*, 539–556 (DOI: 10.1016/j.jasms.2008.11.012).
- (50) Borges, C. R.; Jarvis, J. W.; Oran, P. E.; Nelson, R. W. *J. Proteome Res.* **2008**, *7*, 4143–4153.
- (51) Borges, C. R.; Jarvis, J. W.; Oran, P. E.; Rogers, S. P.; Nelson, R. W. *J. Biomol. Technol.* **2008**, *19*, 167–176.

## SUPPORTING INFORMATION

### Multiplexed Surrogate Analysis of Glycotransferase Activity in Whole Biospecimens

Chad R. Borges<sup>1,\*</sup>, Douglas S. Rehder<sup>1</sup>, and Paolo Boffetta<sup>2</sup>

<sup>1</sup>Molecular Biomarkers Unit, The Biodesign Institute at Arizona State University, Tempe, AZ 85287

<sup>2</sup>Institute for Translational Epidemiology and Tisch Cancer Institute, Mount Sinai School of Medicine, New York, NY 10029

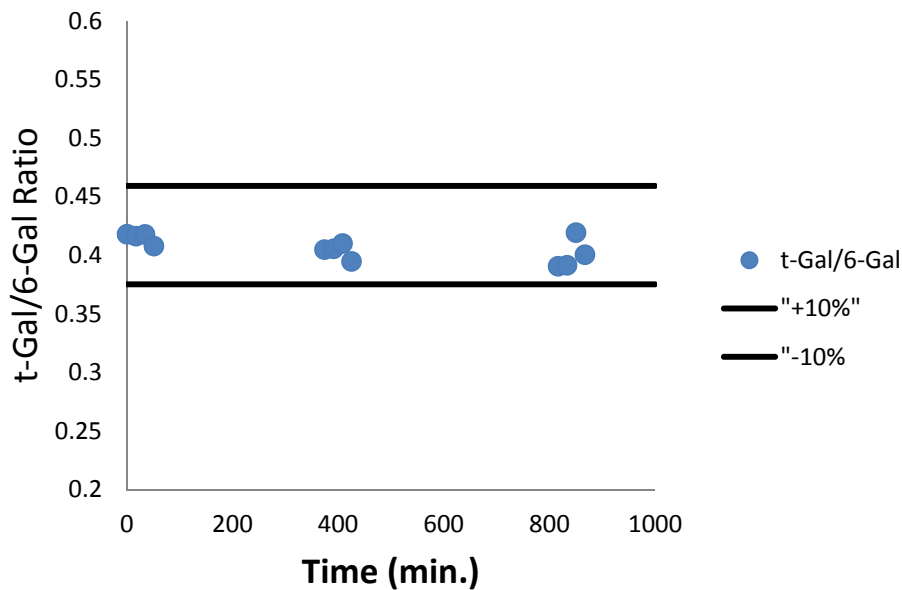
\*Author to whom correspondence should be addressed: Chad R. Borges, Molecular Biomarkers Unit, The Biodesign Institute at Arizona State University, P.O. Box 876601, Tempe, AZ 85287. Tel 480-727-9929, fax 480-727-9464; email: [chad.borges@asu.edu](mailto:chad.borges@asu.edu)

**Contents:** Materials in Supporting Information provide additional details on analytical validation (Figures S1-S3; Tables S5-S7), methodology (Table S1), background information (Tables S2-S4), and clinical verification / disease specificity (Figure S4; Tables S8-S10).

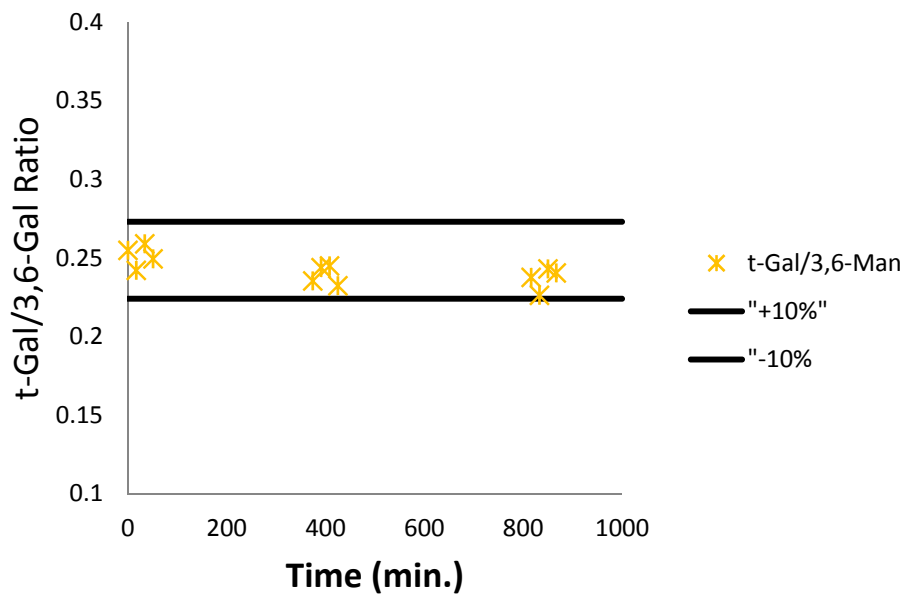
**Abbreviations:** Glycotransferase enzymes (GTs), individual glycan node (iGN), glycan node ratio (GNR), gas chromatograph-mass spectrometry (GC-MS), Lung Cancer in Central and Eastern Europe Study (CEE), receiver operating characteristic (ROC), normal glucose tolerance (NGT), impaired glucose tolerance (IGT), type 2 diabetes (T2D), cardiovascular disease (CVD)

**Supporting Information Figure S1:** Autosampler stability for the top 12 performing glycan node ratios (GNRs) over the time span required to inject 48 samples—the largest batch size employed during analysis of the samples reported in this paper. Passing stability was designated to be within 10% of the average of the first two data points.

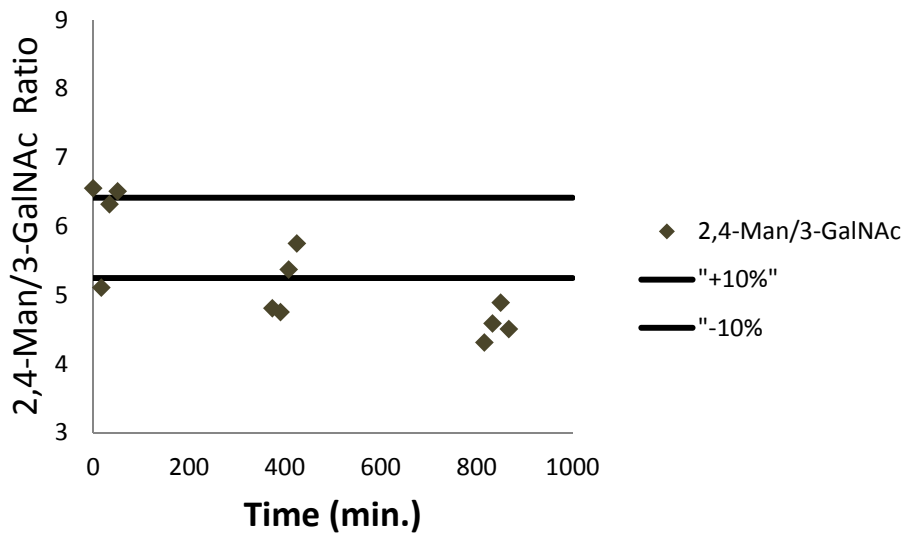
### t-Gal/6-Gal Autosampler Stability



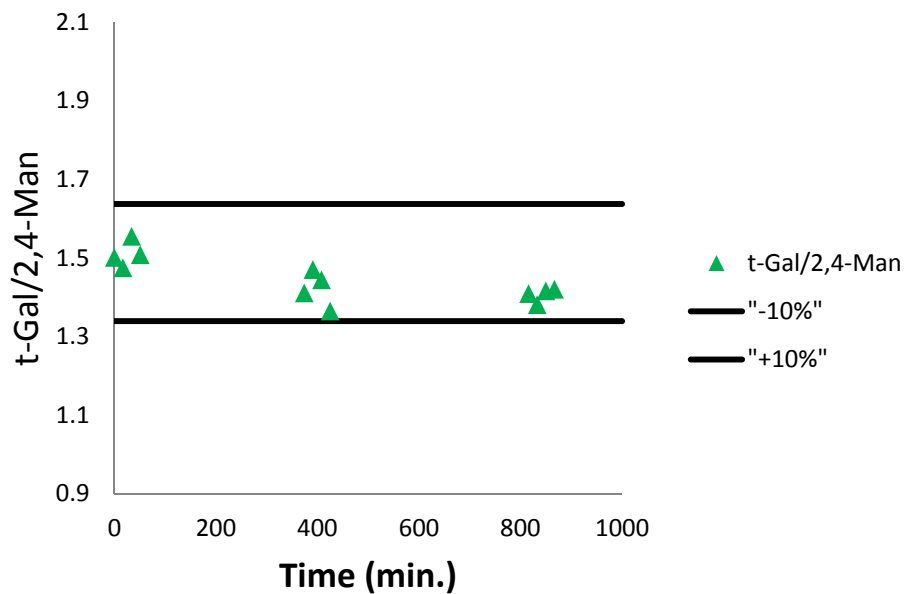
### t-Gal/3,6-Gal Autosampler Stability



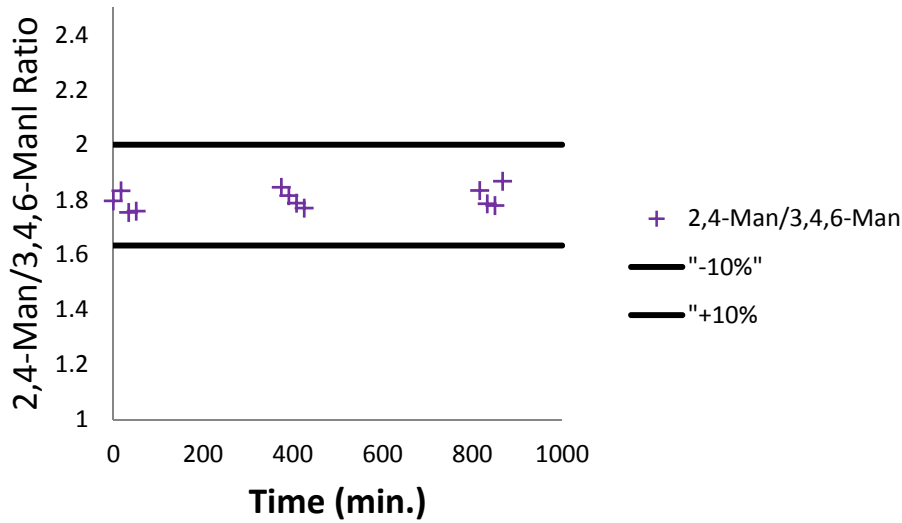
### 2,4-Man/3-GalNAc Autosampler Stability - FAIL



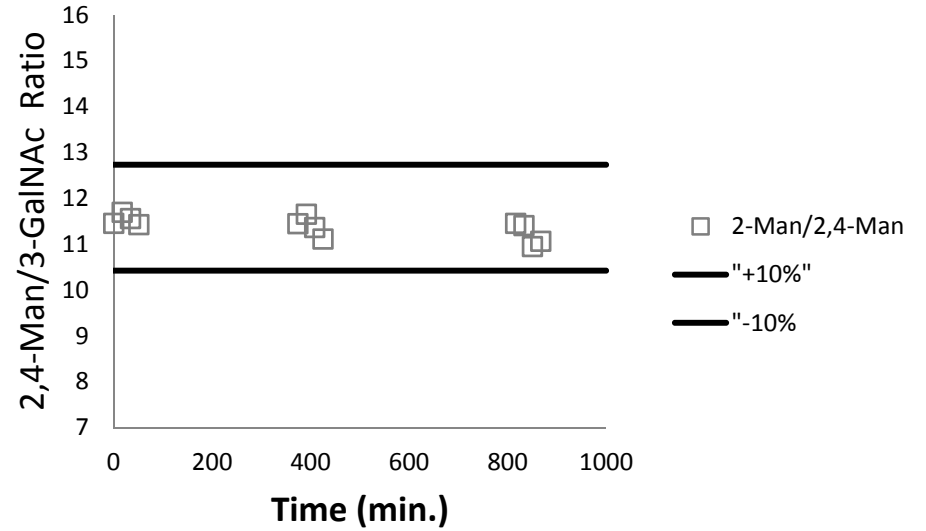
### t-Gal/2,4-Man Autosampler Stability



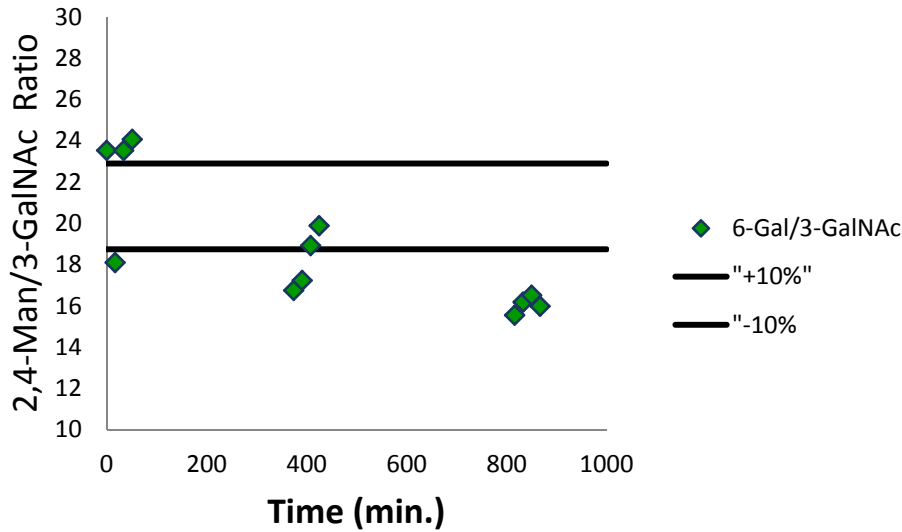
### 2,4-Man/3,4,6-Man Autosampler Stability



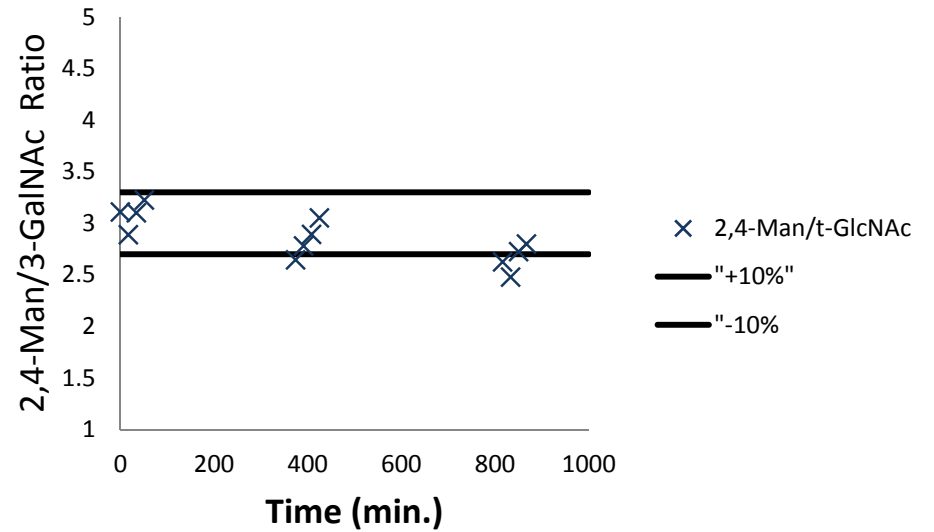
### 2-Man/2,4-Man Autosampler Stability



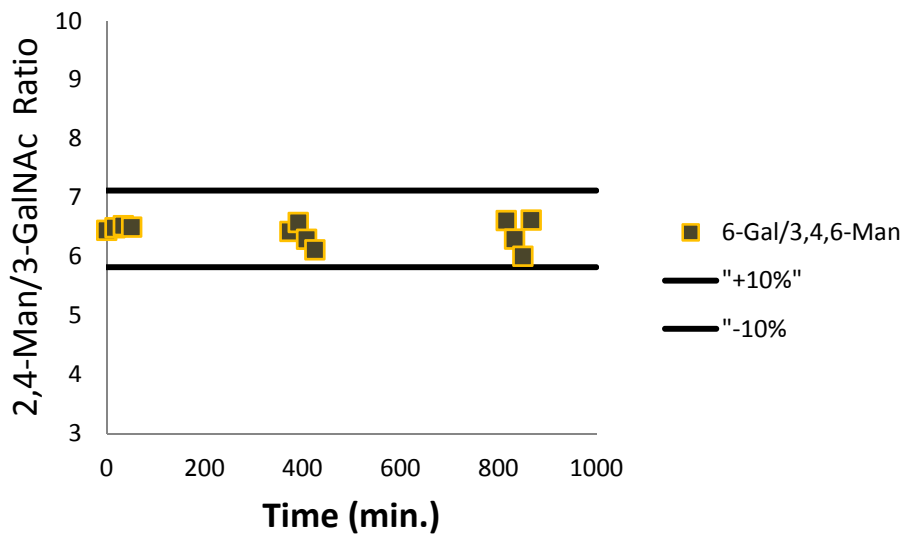
### 6-Gal/3-GalNAc Autosampler Stability - FAIL



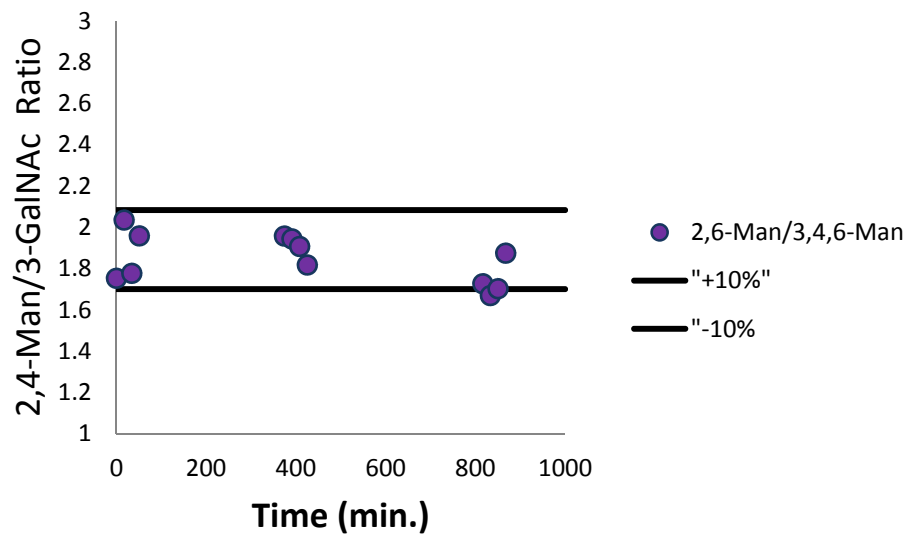
### 2,4-Man/t-GlcNAc Autosampler Stability - FAIL



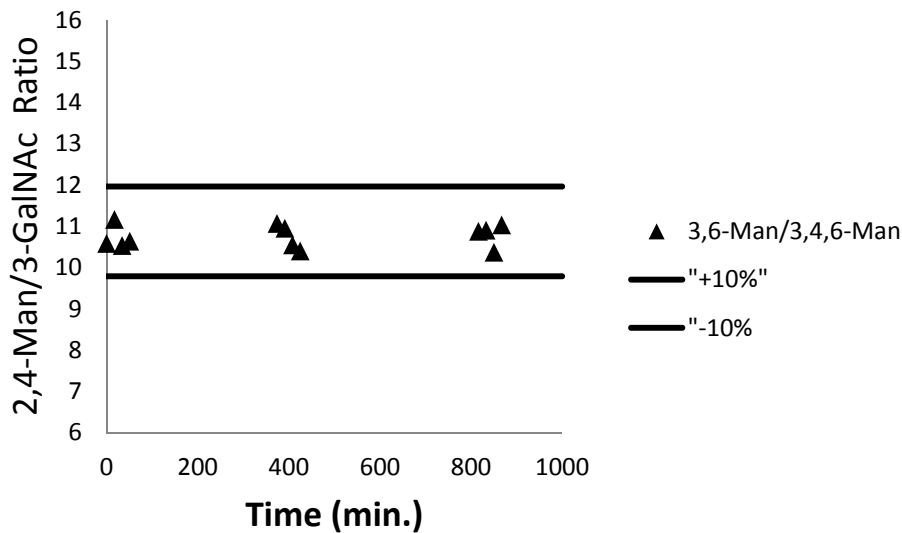
### 6-Gal/3,4,6-Man Autosampler Stability



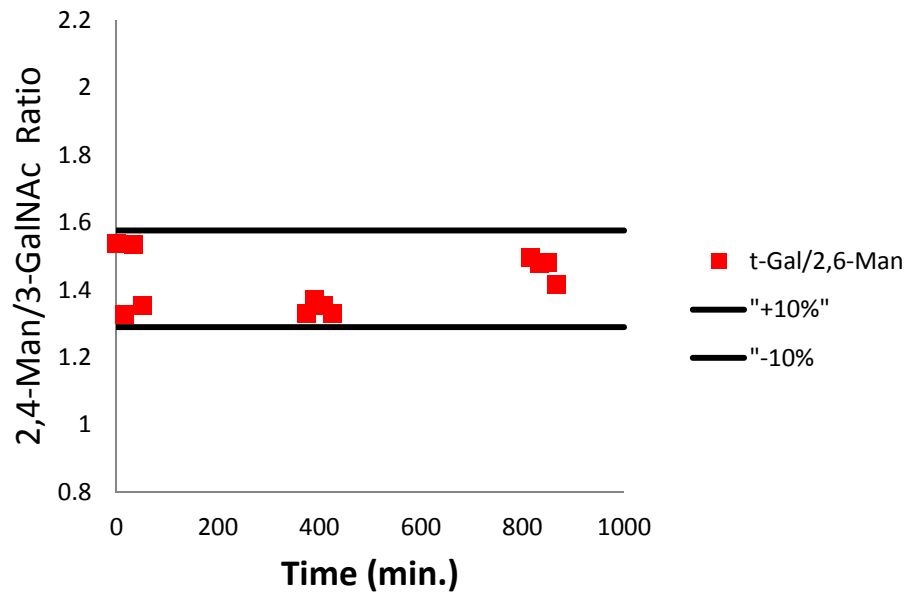
### 2,6-Man/3,4,6-Man Autosampler Stability



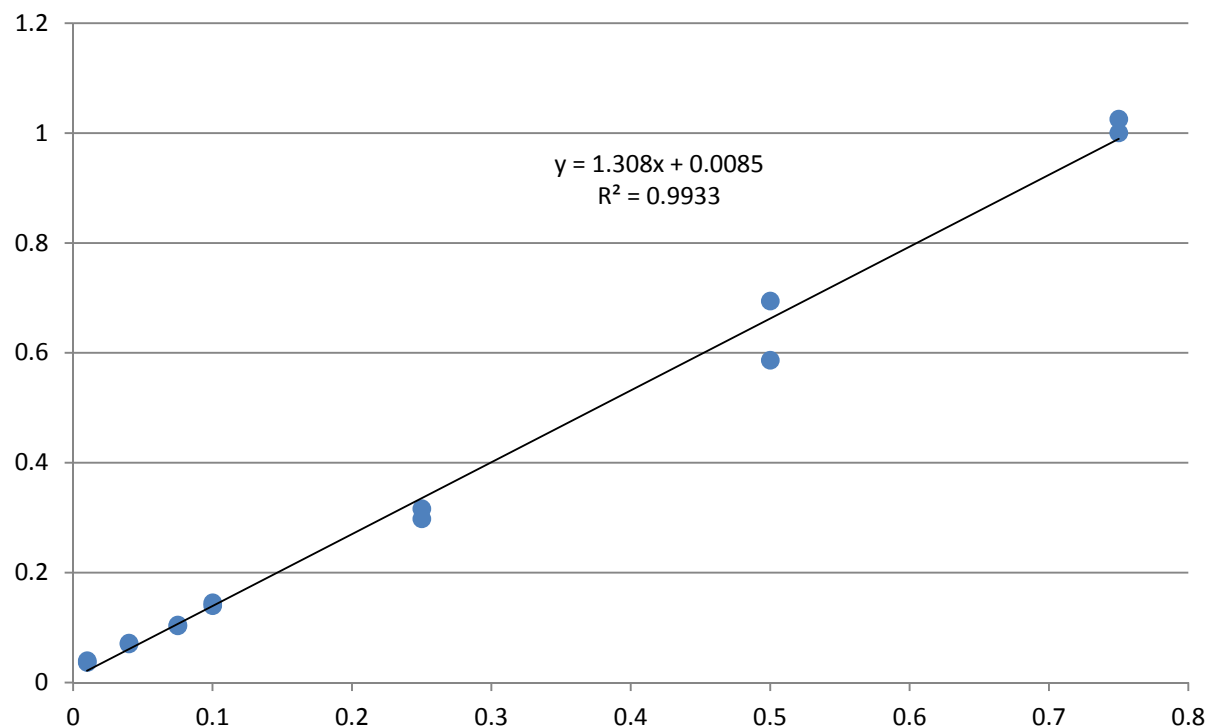
### 3,6-Man/3,4,6-Man Autosampler Stability



### t-Gal/2,6-Man Autosampler Stability

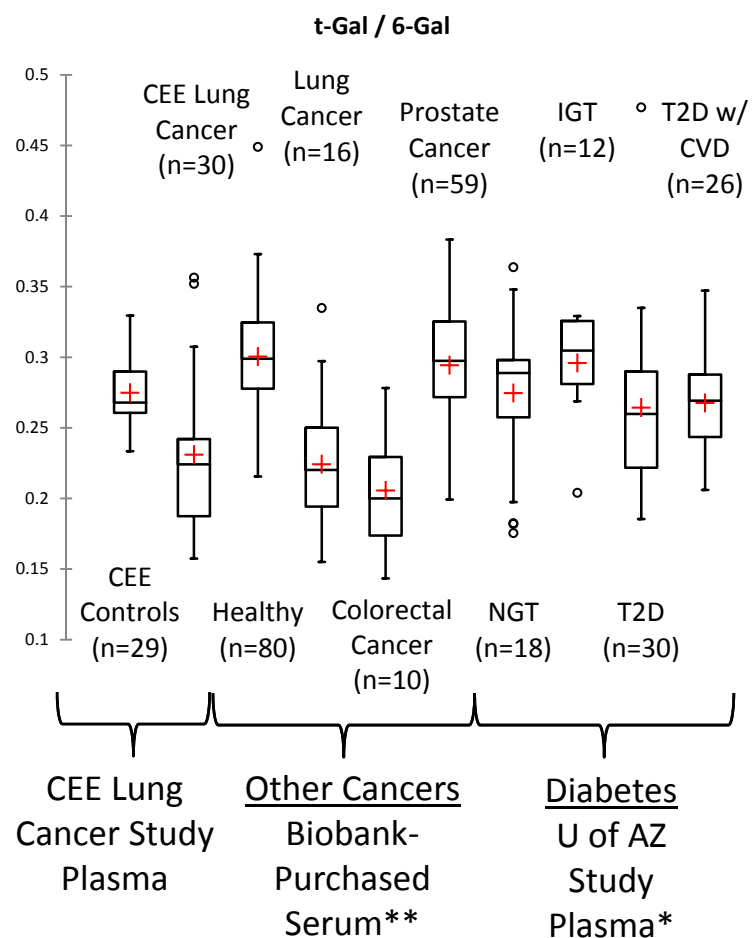


**Response Ratio of t-Gal / 6-Gal vs. Molar Ratio of t-Gal / 6-Gal**



**Supporting Information Figure S2:** Instrument response ratio of t-Gal/6-Gal vs. actual molar ratio of t-Gal/6-Gal. Standards of N-acetyllactosamine (Gal1-4GalNAc) and 6-Sialyl-N-acetyllactosamine (NeuNAc2-6Gal1-4GalNAc) were employed to construct this curve. Overall signal intensities approximated those from blood plasma samples. Data points represent two standard curves run on two separate days. Extracted ion chromatograms for calculating instrument response ratio are found in Supporting Information Table S1.

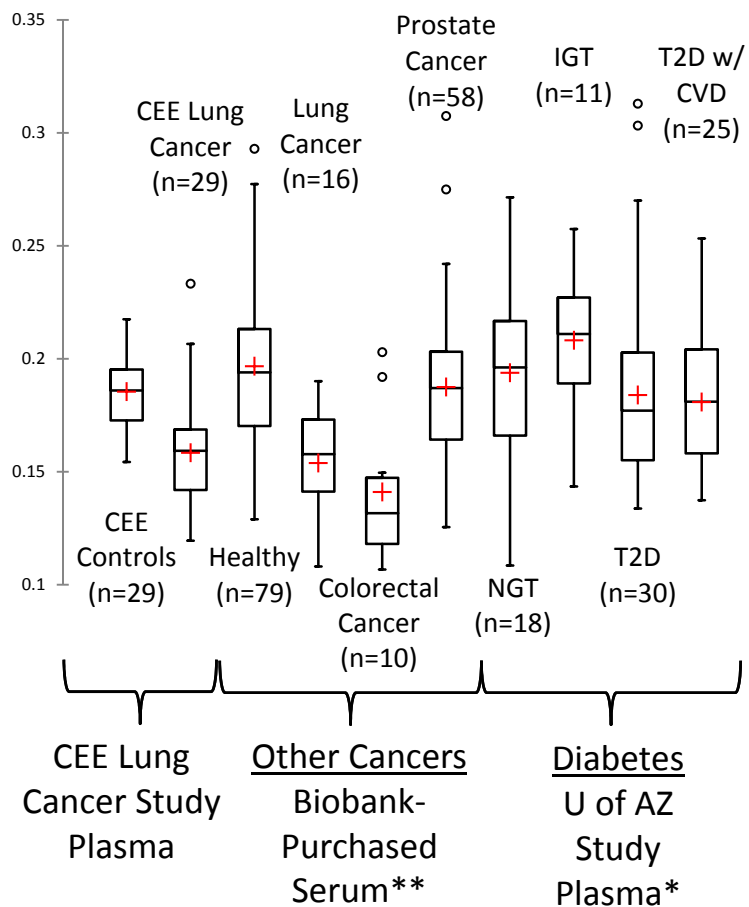




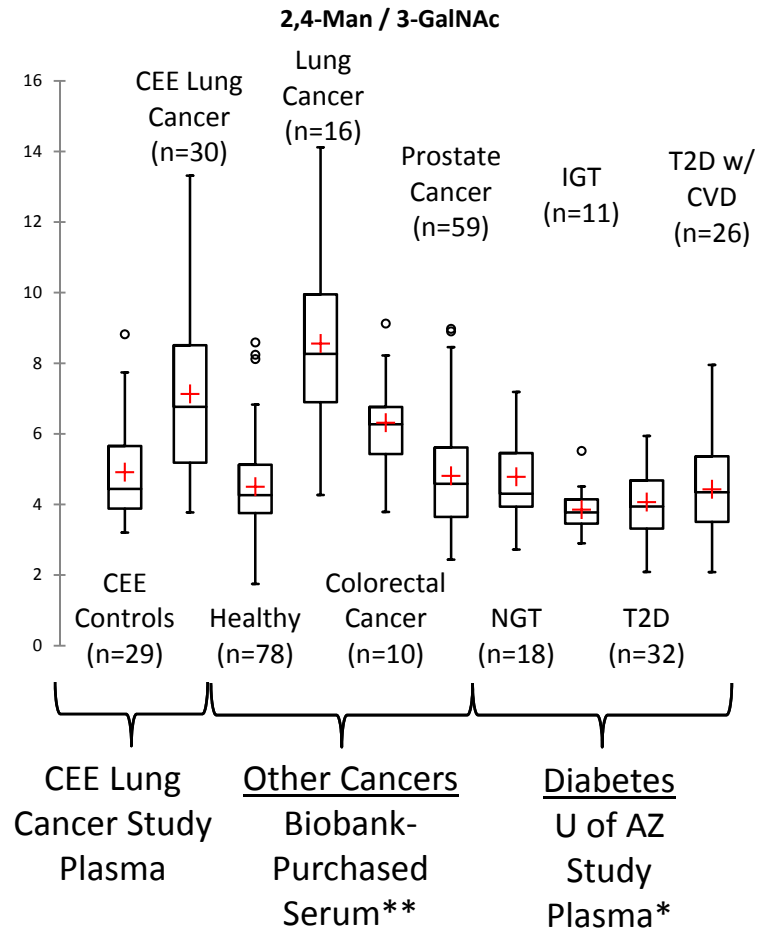
| Category                  | LS means | Groups |   |
|---------------------------|----------|--------|---|
| Biobank Healthy           | 0.300    | A      |   |
| IGT                       | 0.296    | A      |   |
| Biobank Prostate Cancer   | 0.294    | A      |   |
| CEE Controls              | 0.275    | A      | B |
| NGT                       | 0.275    | A      | B |
| T2D w/ CVD                | 0.268    |        | B |
| T2D                       | 0.264    |        | B |
| CEE Lung Cancer           | 0.231    |        | C |
| Biobank Lung Cancer       | 0.224    |        | C |
| Biobank Colorectal Cancer | 0.206    |        | C |

**Supporting Information Figures S3:** Cancer and chronic disease specificity cross-check for the top 6 performing GNRs in the CEE lung cancer cohort. Statistically significant differences between groups (calculated by ANOVA followed by the Ryan-Einot-Gabriel-Welsch multiple comparison test) are indicated in the adjoining tables at right: Lack of overlap in assigned letters indicates statistical significance; any overlap in an assigned letter indicates lack of a statistically significant difference. As reflected in the n-values, between two and seven extreme outliers from various groups were removed per box-plot / ANOVA comparison. \*Diabetes Category Abbreviations: NGT = Normal Glucose Tolerance (Healthy), IGT = Impaired Glucose Tolerance (Pre-T2D), T2D = Type 2 Diabetes, T2D w/ CVD = Type 2 Diabetes with cardiovascular complications. \*\*As described in the manuscript, a pre-analytics study of matched collections of serum and 4 types of plasma show no significant differences in these GNRs.

**t-Gal / 3,6-Man**

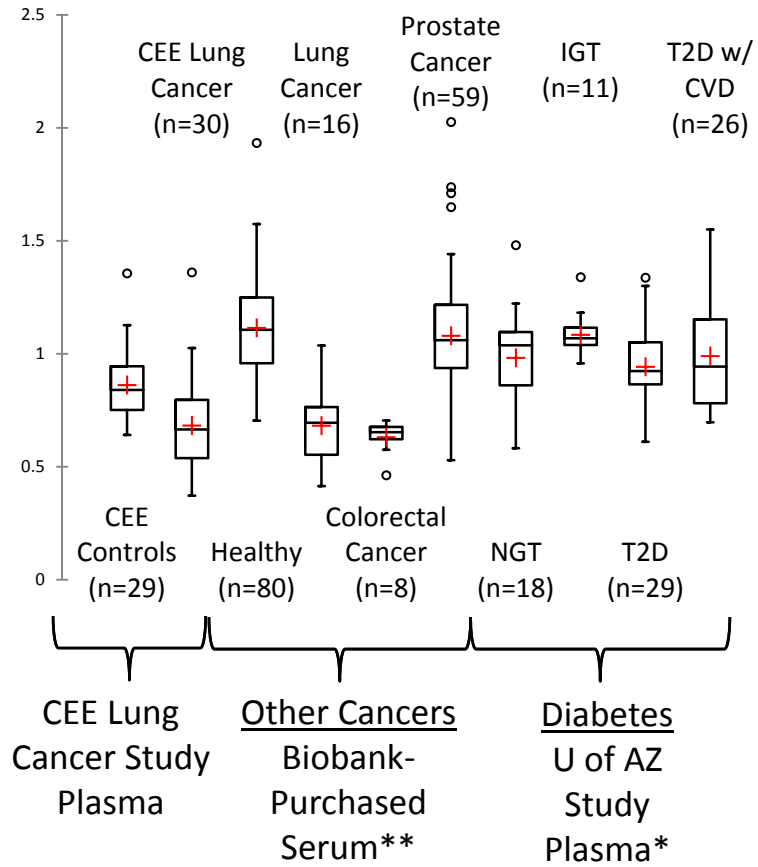


| Category                  | LS means | Groups |   |
|---------------------------|----------|--------|---|
| IGT                       | 0.208    | A      |   |
| Biobank Healthy           | 0.197    | A      |   |
| NGT                       | 0.194    | A      |   |
| Biobank Prostate Cancer   | 0.187    | A      |   |
| CEE Controls              | 0.185    | A      |   |
| T2D                       | 0.184    | A      |   |
| T2D w/ CVD                | 0.181    | A      | B |
| CEE Lung Cancer           | 0.158    | B      | C |
| Biobank Lung Cancer       | 0.154    | B      | C |
| Biobank Colorectal Cancer | 0.141    |        | C |



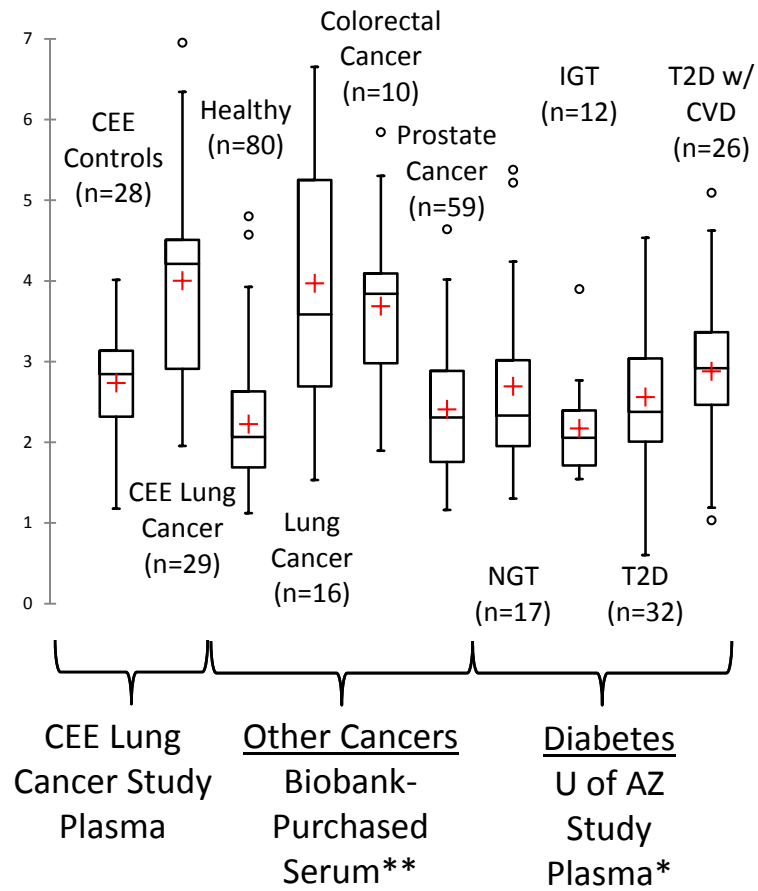
| Category                  | LS means | Groups |   |   |
|---------------------------|----------|--------|---|---|
| Biobank Lung Cancer       | 8.560    | A      |   |   |
| CEE Lung Cancer           | 7.129    |        | B |   |
| Biobank Colorectal Cancer | 6.313    |        | B | C |
| CEE Controls              | 4.912    |        |   | C |
| Biobank Prostate Cancer   | 4.808    |        |   | C |
| NGT                       | 4.785    |        |   | C |
| Biobank Healthy           | 4.500    |        |   | D |
| T2D w/ CVD                | 4.428    |        |   | D |
| T2D                       | 4.067    |        |   | D |
| IGT                       | 3.851    |        |   | D |

**t-Gal / 2,4-Man**

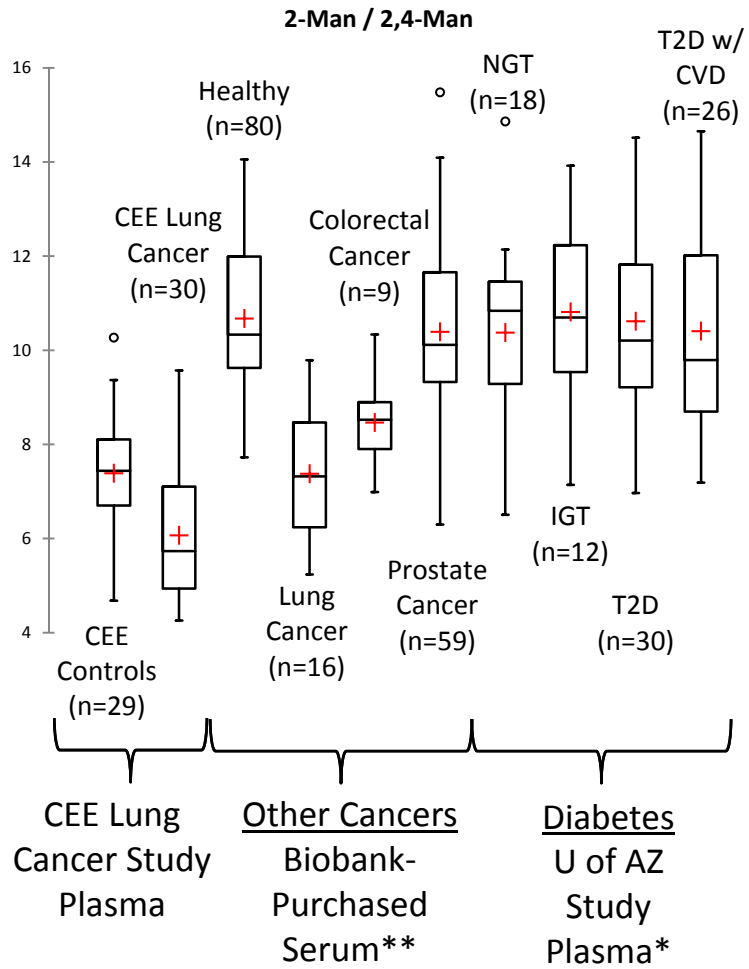


| Category                  | LS means | Groups |
|---------------------------|----------|--------|
| Biobank Healthy           | 1.114    | A      |
| IGT                       | 1.084    | A      |
| Biobank Prostate Cancer   | 1.080    | A      |
| T2D w/ CVD                | 0.989    | A B    |
| NGT                       | 0.982    | A B    |
| T2D                       | 0.942    | B      |
| CEE Controls              | 0.861    | B      |
| CEE Lung Cancer           | 0.682    | C      |
| Biobank Lung Cancer       | 0.681    | C      |
| Biobank Colorectal Cancer | 0.631    | C      |

**2,4-Man / 3,4,6-Man**



| Category                  | LS means | Groups |   |
|---------------------------|----------|--------|---|
| CEE Lung Cancer           | 4.002    | A      |   |
| Biobank Lung Cancer       | 3.970    | A      |   |
| Biobank Colorectal Cancer | 3.687    | A      |   |
| T2D w/ CVD                | 2.879    | B      |   |
| CEE Controls              | 2.734    | B      | C |
| NGT                       | 2.694    | B      | C |
| T2D                       | 2.560    | B      | C |
| Biobank Prostate Cancer   | 2.407    | B      | C |
| Biobank Healthy           | 2.225    |        | C |
| IGT                       | 2.172    |        | C |



| Category                  | LS means | Groups |   |
|---------------------------|----------|--------|---|
| IGT                       | 10.814   | A      |   |
| Biobank Healthy           | 10.673   | A      |   |
| T2D                       | 10.616   | A      |   |
| T2D w/ CVD                | 10.406   | A      |   |
| Biobank Prostate Cancer   | 10.391   | A      |   |
| NGT                       | 10.375   | A      |   |
| Biobank Colorectal Cancer | 8.464    | B      |   |
| CEE Controls              | 7.387    | B      |   |
| Biobank Lung Cancer       | 7.375    | B      | C |
| CEE Lung Cancer           | 6.069    |        | C |

**Supporting Information Table S1:** Blood plasma/serum data processing parameters. The indicated extracted ion chromatograms (XICs) are summed and automatically integrated by QuanLynx software, manually verified and exported to a spreadsheet.

| <u>PMAA Analyte<sup>a</sup></u> | <u>Summed Ion XIC<sup>b</sup></u> | <u>Retention Time (min.)</u> |
|---------------------------------|-----------------------------------|------------------------------|
| Heavy Fucose                    | 119.06+134.08                     | 4.13                         |
| t-Fuc                           | 117.05+131.05                     | 4.13                         |
| Heavy Glucose                   | 135.05+153.1+168.1                | 4.93                         |
| t-Glc &/or t-Man                | 117.05+145.1                      | 4.98                         |
| t-Gal                           | 117.05+145.1                      | 5.15                         |
| 2-Man                           | 129.05+189.1                      | 5.72                         |
| 4-Gal/4-Man                     | 113.05+117.05+233.1               | 5.77                         |
| 4-Glc                           | 113.05+117.05+233.1               | 5.83                         |
| 3-Man                           | 117.05                            | 5.87                         |
| 2-Gal                           | 189.1                             | 5.89                         |
| 3-Gal                           | 117.05+161.1+233.1                | 5.95                         |
| 6-Glc &/or 6-Man                | 117.05+129.05                     | 6.03                         |
| 6-Gal                           | 117.05+161.1+233.1                | 6.31                         |
| 3,4-Gal                         | 117.05                            | 6.38                         |
| 2,3-Gal                         | 161.08+261.09                     | 6.53                         |
| 2,4-Man                         | 129.05+189.1+233.1                | 6.55                         |
| 4,6-Glc                         | 117.08+129.08+261.09              | 6.78                         |
| 2,6-Man                         | 129.05+189.1                      | 6.86                         |
| 3,6-Man                         | 117.05+129.05+189.1+233.1         | 7.00                         |
| 3,6-Gal                         | 117.05+129.05+189.1+233.1         | 7.13                         |
| 3,4,6-Man                       | 117.05+139.05+333.12              | 7.31                         |
| Heavy GlcNAc                    | 118.08+160.09                     | 7.71                         |
| t-GlcNAc                        | 116.08+158.08                     | 7.71                         |
| t-GalNAc                        | 116.08+158.08                     | 8.04                         |
| 4-GlcNAc                        | 158.08                            | 8.34                         |
| 3-GlcNAc                        | 116.08+158.08                     | 8.69                         |
| 3-GalNAc                        | 116.08+158.08                     | 8.79                         |
| 6-GlcNAc                        | 116.08+158.08                     | 8.84                         |
| 3,4-GlcNAc                      | 116.08+158.08                     | 8.99                         |
| 4-GalNAc                        | 116.08+158.08                     | 9.08                         |
| 6-GalNAc                        | 116.08+158.08                     | 9.15                         |
| 4,6-GlcNAc                      | 116.08+158.08                     | 9.37                         |
| 3,6-GalNAc                      | 116.08+158.08                     | 9.89                         |

<sup>a</sup> PMAA = Partially Methylated Alditol Acetate. "t-" indicates a terminal residue and "n-", "n,n-", or "n,n,n-" indicate linkage positions of the residue in the original glycan polymer. Monosaccharide abbreviations are provided in Fig. 1.

<sup>b</sup> XIC = Extracted Ion Chromatogram. A mass window of  $\pm 0.15$  Da is taken around the indicated  $m/z$











**Supporting Information Table S3:** Clinical characteristics and the risk of lung cancer mortality in the Lung Cancer in Central and Eastern Europe study.

|                         | Total Patients | Deaths | HR*  | CI         | 5-year survival | Median survival (months) |
|-------------------------|----------------|--------|------|------------|-----------------|--------------------------|
| <u>Grade</u>            |                |        |      |            |                 |                          |
| Grade 1                 | 29             | 18     | ref  |            | 0.48            | 43.5                     |
| Grade 2                 | 83             | 68     | 1.89 | 1.11, 3.21 | 0.23            | 18.0                     |
| Grade 3                 | 114            | 101    | 2.57 | 1.54, 4.28 | 0.16            | 17.3                     |
| Grade 4                 | 55             | 51     | 3.29 | 1.90, 5.70 | 0.09            | 11.9                     |
| not applicable          | 604            | 531    | 2.88 | 1.75, 4.73 | 0.15            | 15.0                     |
| missing                 | 950            | 714    |      |            |                 |                          |
| <u>Histology</u>        |                |        |      |            |                 |                          |
| Squamous cell carcinoma | 713            | 586    | ref  |            | 0.22            | 15.9                     |
| Small cell carcinoma    | 360            | 312    | 1.24 | 1.07, 1.43 | 0.15            | 14.9                     |
| Adenocarcinoma          | 387            | 282    | 0.94 | 0.82, 1.09 | 0.31            | 21.9                     |
| Large cell carcinoma    | 55             | 41     | 1.08 | 0.77, 1.49 | 0.3636          | 20.5                     |
| Mixed                   | 73             | 50     | 0.70 | 0.52, 0.94 | 0.33            | 24.4                     |
| Other/Unspecified       | 245            | 210    | 1.22 | 1.04, 1.45 | 0.19            | 12.9                     |
| <u>TNM stage</u>        |                |        |      |            |                 |                          |
| 1                       | 96             | 59     | ref  |            | 0.54            | 79.0                     |
| 2                       | 75             | 60     | 1.93 | 1.34, 2.77 | 0.28            | 21.7                     |
| 3                       | 305            | 281    | 3.16 | 2.36, 4.22 | 0.09            | 15.7                     |
| 4                       | 287            | 265    | 3.85 | 2.87, 5.16 | 0.08            | 12.3                     |

Abbreviations: HR = hazard ratios, adjusted for the variable in the table; CI = confidence intervals; ref = reference category.

Supporting Information Table S4: Individual patient details from the Lung Cancer in Central and Eastern Europe (CEE) Study

| Lung Cancer Case or Control | Gender | Age (yrs.) | Type of Smoker | Age at which Started Smoking | Average Daily Tobacco Consumption (# of cigarettes) | Cumulative Smoking History (Tobacco pack yrs.) | Age at which Quit Smoking | Time Since Quit Smoking | Type of Tobacco (1=Never smoker, 2=Cigarettes only, 3=Never cigarettes, 4=Cigarettes + other) | Lung Histology (0=controls 1=Adenocarcinoma, 2=Squamous cell carcinoma, 3=Small cell, 4=Others/mixed) |
|-----------------------------|--------|------------|----------------|------------------------------|---|--|---------------------------|-------------------------|---|---|
| Control                     | Female | 59         | Never Smoker   |                              | 0.0   | 0.0  |                           |                         | 1   | 0   |
| Control                     | Female | 70         | Never Smoker   |                              | 0.0   | 0.0  |                           |                         | 1   | 0   |
| Lung Cancer                 | Male   | 41         | Current Smoker | 21                           | 20.0  | 20.0   |                           | 0                       | 2   | 2   |
| Lung Cancer                 | Female | 46         | Ex-Smoker      | 18                           | 14.5  | 16.0   | 40.0                      | 6                       | 2   | 1   |
| Lung Cancer                 | Female | 66         | Ex-Smoker      | 25                           | 5.0   | 8.8  | 60.0                      | 6                       | 2   | 1   |
| Lung Cancer                 | Female | 65         | Current Smoker | 23                           | 48.6  | 102.0  | 65.0                      | 0                       | 2   | 4   |
| Lung Cancer                 | Female | 68         | Current Smoker | 25                           | 17.6  | 37.0   | 67.0                      | 1                       | 2   | 4   |
| Lung Cancer                 | Male   | 68         | Ex-Smoker      | 20                           | 15.0  | 15.0   | 40.0                      | 28                      | 2   | 2   |
| Control                     | Male   | 58         | Current Smoker | 26                           | 12.0  | 19.2   |                           | 0                       | 2   | 0   |
| Control                     | Female | 73         | Current Smoker | 34                           | 24.6  | 48.0   |                           | 0                       | 2   | 0   |
| Control                     | Male   | 69         | Ex-Smoker      | 25                           | 10.0  | 12.0   | 49.0                      | 20                      | 2   | 0   |
| Control                     | Female | 62         | Current Smoker | 30                           | 9.3   | 14.9   |                           | 0                       | 2   | 0   |
| Lung Cancer                 | Male   | 44         | Ex-Smoker      | 17                           | 17.1  | 18.0   | 38.0                      | 6                       | 2   | 4   |
| Lung Cancer                 | Male   | 64         | Ex-Smoker      | 19                           | 20.0  | 39.0   | 58.0                      | 6                       | 2   | 4   |
| Control                     | Female | 52         | Current Smoker | 25                           | 10.0  | 13.5   |                           | 0                       | 2   | 0   |
| Control                     | Female | 70         | Never Smoker   |                              | 0.0   | 0.0  |                           |                         | 1   | 0   |
| Control                     | Female | 50         | Never Smoker   |                              | 0.0   | 0.0  |                           |                         | 1   | 0   |
| Control                     | Female | 60         | Current Smoker | 19                           | 18.8  | 38.5   |                           | 0                       | 2   | 0   |
| Lung Cancer                 | Female | 51         | Current Smoker | 19                           | 16.6  | 26.5   | 51.0                      | 0                       | 2   | 1   |
| Control                     | Female | 58         | Current Smoker | 17                           | 16.5  | 33.9   |                           | 0                       | 2   | 0   |
| Control                     | Male   | 56         | Never Smoker   |                              | 0.0   | 0.0  |                           |                         | 1   | 0   |
| Lung Cancer                 | Female | 65         | Current Smoker | 18                           | 15.0  | 35.3   | 65.0                      | 0                       | 2   | 4   |
| Lung Cancer                 | Male   | 71         | Ex-Smoker      | 12                           | 17.3  | 45.0   | 64.0                      | 7                       | 2   | 2   |
| Lung Cancer                 | Female | 72         | Never Smoker   |                              | 0.0   | 0.0  |                           |                         | 1   | 2   |
| Control                     | Male   | 67         | Current Smoker | 18                           | 14.7  | 36.8   |                           | 0                       | 2   | 0   |
| Control                     | Male   | 71         | Current Smoker | 20                           | 17.1  | 43.7   |                           | 0                       | 4   | 0   |
| Lung Cancer                 | Female | 45         | Never Smoker   |                              | 0.0   | 0.0  |                           |                         | 1   | 4   |
| Control                     | Male   | 63         | Current Smoker | 17                           | 10.1  | 23.3   |                           | 0                       | 4   | 0   |
| Lung Cancer                 | Male   | 70         | Ex-Smoker      | 15                           | 22.8  | 40.0   | 50.0                      | 20                      | 4   | 2   |
| Lung Cancer                 | Male   | 60         | Current Smoker | 20                           | 18.0  | 36.0   |                           | 0                       | 2   | 2   |
| Lung Cancer                 | Female | 74         | Current Smoker | 20                           | 19.9  | 53.6   |                           | 0                       | 4   | 4   |
| Lung Cancer                 | Male   | 51         | Current Smoker | 10                           | 17.4  | 35.7   |                           | 0                       | 4   | 1   |
| Lung Cancer                 | Female | 70         | Never Smoker   |                              | 0.0   | 0.0  |                           |                         | 1   | 4   |
| Lung Cancer                 | Male   | 58         | Current Smoker | 20                           | 15.9  | 30.9   |                           | 0                       | 4   | 2   |
| Lung Cancer                 | Male   | 56         | Current Smoker | 17                           | 14.0  | 27.3   |                           | 0                       | 2   | 2   |
| Control                     | Male   | 61         | Current Smoker | 8                            | 10.0  | 26.5   |                           | 0                       | 2   | 0   |
| Control                     | Male   | 77         | Ex-Smoker      | 18                           | 6.8   | 3.7  | 29.0                      | 48                      | 3   | 0   |
| Control                     | Male   | 68         | Ex-Smoker      | 16                           | 10.5  | 11.6   | 38.0                      | 30                      | 3   | 0   |
| Control                     | Female | 64         | Never Smoker   |                              | 0.0   | 0.0  |                           |                         | 1   | 0   |
| Control                     | Male   | 72         | Ex-Smoker      | 17                           | 10.5  | 4.2  | 25.0                      | 47                      | 3   | 0   |
| Control                     | Male   | 71         | Current Smoker | 20                           | 9.3   | 23.6   |                           | 0                       | 4   | 0   |
| Control                     | Male   | 69         | Current Smoker | 22                           | 20.0  | 47.0   |                           | 0                       | 2   | 0   |
| Lung Cancer                 | Male   | 68         | Ex-Smoker      | 21                           | 10.0  | 6.0  | 33.0                      | 35                      | 2   | 2   |
| Lung Cancer                 | Female | 73         | Ex-Smoker      | 22                           | 9.9   | 10.9   | 44.0                      | 29                      | 2   | 1   |
| Lung Cancer                 | Male   | 53         | Current Smoker | 15                           | 11.7  | 22.3   |                           | 0                       | 2   | 2   |
| Lung Cancer                 | Male   | 45         | Current Smoker | 15                           | 19.6  | 29.4   |                           | 0                       | 2   | 1   |
| Lung Cancer                 | Male   | 68         | Ex-Smoker      | 24                           | 7.1   | 11.4   | 56.0                      | 12                      | 4   | 1   |
| Control                     | Male   | 68         | Current Smoker | 13                           | 10.5  | 28.9   |                           | 0                       | 3   | 0   |
| Control                     | Male   | 61         | Ex-Smoker      | 15                           | 15.0  | 11.3   | 30.0                      | 31                      | 2   | 0   |
| Lung Cancer                 | Female | 46         | Ex-Smoker      | 18                           | 14.5  | 16.0   | 40.0                      | 6                       | 2   | 1   |
| Control                     | Female | 55         | Current Smoker | 20                           | 8.0   | 14.0   |                           | 0                       | 2   | 0   |
| Control                     | Female | 49         | Ex-Smoker      | 16                           | 9.2   | 10.1   | 38.0                      | 11                      | 2   | 0   |
| Control                     | Female | 54         | Ex-Smoker      | 20                           | 3.0   | 1.5  | 30.0                      | 24                      | 2   | 0   |
| Lung Cancer                 | Female | 48         | Current Smoker | 20                           | 6.0   | 8.4  | 48.0                      | 0                       | 2   | 1   |
| Control                     | Male   | 68         | Ex-Smoker      | 22                           | 13.6  | 19.0   | 50.0                      | 18                      | 2   | 0   |
| Lung Cancer                 | Female | 52         | Current Smoker | 20                           | 17.7  | 28.3   | 52.0                      | 0                       | 2   | 3   |
| Lung Cancer                 | Male   | 70         | Current Smoker | 20                           | 19.6  | 50.0   |                           | 0                       | 2   | 2   |
| Control                     | Female | 54         | Current Smoker | 25                           | 12.0  | 17.4   |                           | 0                       | 2   | 0   |
| Lung Cancer                 | Male   | 72         | Ex-Smoker      | 15                           | 20.0  | 41.0   | 56.0                      | 16                      | 2   | 2   |

**Supporting Information Table S5:** Clinical and analytical performance of individual glycan nodes (iGNs). Left-hand columns provide statistical comparisons of cancer cases (n = 30) vs. controls (n = 26)<sup>a</sup> in the CEE Lung Cancer cohort. Raw data from which these values were calculated were the ratio of glycan node peak area / stable-isotope-labeled-monosaccharide-internal-standard peak area. All iGNs showed an increasing trend in the cancer patient samples, even if there was not a statistically significant difference. Right-hand columns illustrate the relatively poor intra- and inter-assay precision<sup>b</sup> of iGNs (indicated by grey cells). This analytical feature probably contributed to the weaker diagnostic performance of iGNs relative to GNRs (Table 1): Despite strong statistical significance, none of these iGNs produced an ROC c-statistic of over 0.75.

|                  | CEE Lung Cancer vs. CEE Controls t-test p-value <sup>b</sup> | ROC c-statistic (AUC ± SE) | Intra-Assay Precision (%CV) | Inter-Assay Precision (%CV) |
|------------------|--|----------------------------|-----------------------------|-----------------------------|
| t-Fuc            | 0.0022   | 0.697 ± 0.067              | 14.89                       | 27.66                       |
| t-Gal            | 0.0398   | 0.643 ± 0.072              | 16.22                       | 28.51                       |
| 2-Man            | 0.0116   | 0.663 ± 0.070              | 18.69                       | 27.14                       |
| 4-Glc            | 0.6773   | NS <sup>d</sup>            | 37.46                       | 61.07                       |
| 3-Gal            | 0.00204  | 0.713 ± 0.066              | 14.91                       | 28.23                       |
| 6-Glc &/or 6-Man | 0.178  | NS <sup>d</sup>            | 24.29                       | 34.62                       |
| 6-Gal            | 0.00086  | 0.737 ± 0.064              | 16.69                       | 29.15                       |
| 3,4-Gal          | 0.0064   | 0.679 ± 0.069              | 27.75                       | 35.4                        |
| 2,4-Man          | 0.00034  | 0.747 ± 0.063              | 18.72                       | 30.88                       |
| 2,6-Man          | 0.00099  | 0.731 ± 0.065              | 18.96                       | 27.64                       |
| 3,6-Man          | 0.00142  | 0.719 ± 0.065              | 15.15                       | 25.17                       |
| 3,6-Gal          | 0.0125   | 0.697 ± 0.068              | 22.49                       | 37.86                       |
| 3,4,6-Man        | 0.213  | NS <sup>d</sup>            | 16.58                       | 24.72                       |
| t-GlcNAc         | 0.205  | NS <sup>d</sup>            | 7.55                        | 9.92                        |
| 4-GlcNAc         | 0.00412  | 0.704 ± 0.069              | 12.03                       | 16.33                       |
| 3-GlcNAc         | 0.43293  | NS <sup>d</sup>            | 30.57                       | 33.08                       |
| 3-GalNAc         | 0.1295   | NS <sup>d</sup>            | 10.74                       | 12.06                       |
| 3,4-GlcNAc       | 0.00245  | 0.713 ± 0.069              | 15.85                       | 17.78                       |
| 4,6-GlcNAc       | 0.07692  | NS <sup>d</sup>            | 13.85                       | 15.21                       |
| 3,6-GalNAc       | 0.23354  | NS <sup>d</sup>            | 27.36                       | 29.63                       |

<sup>a</sup> Data for three control samples are missing because internal standard was mistakenly omitted from them during sample processing.

<sup>b</sup> n = 6 samples analyzed on three different days

<sup>c</sup> Two-sided Student's t-test. GNs for which 0.005 < p < 0.05 are highlighted in light blue; p < 0.005 highlighted in dark yellow.

<sup>d</sup> NS indicates not statistically significant.

**Supporting Information Table S6:** Stability of the top 12 lung cancer glycan node ratios when plasma samples were left at room temperature overnight. Twelve aliquots of the same sample were created and 6 were placed at -80 °C overnight and the remaining 6 were kept out a room temperature. For the two cases in which a statistically significant difference is noted, the overall difference between the sample sets was less than 12%.

| <b>Glycan Node Ratio</b> | <b>Kept in Freezer (Avg. ± SE)</b> | <b>Room Temp. Overnight (Avg. ± SE)</b> | <b>T-Test (p-value)</b> |
|--------------------------|------------------------------------|---|-------------------------|
| t-Gal/6-Gal              | 0.378 ± 0.0106                     | 0.386 ± 0.0108                          | 0.195                   |
| t-Gal/3,6-Man            | 0.221 ± 0.0166                     | 0.223 ± 0.0203                          | 0.877                   |
| 2,4-Man/3-GalNAc         | 4.57 ± 0.629                       | 4.26 ± 0.590                            | 0.426                   |
| t-Gal/2,4-Man            | 1.52 ± 0.118                       | 1.47 ± 0.0777                           | 0.440                   |
| 2,4-Man/3,4,6-Man        | 1.86 ± 0.165                       | 2.05 ± 0.190                            | 0.107                   |
| 2-Man/2,4-Man            | 12.2 ± 0.958                       | 11.6 ± 0.649                            | 0.274                   |
| 6-Gal/3-GalNAc           | 18.2 ± 1.12                        | 16.3 ± 1.33                             | 0.0292                  |
| 2,4-Man/t-GlcNAc         | 2.43 ± 0.165                       | 2.31 ± 0.242                            | 0.405                   |
| 6-Gal/3,4,6-Man          | 7.46 ± 0.297                       | 7.79 ± 0.630                            | 0.287                   |
| 2,6-Man/3,4,6-Man        | 1.87 ± 0.103                       | 1.82 ± 0.163                            | 0.517                   |
| 3,6-Man/3,4,6-Man        | 12.7 ± 0.295                       | 13.5 ± 1.02                             | 0.127                   |
| t-Gal/2,6-Man            | 1.50 ± 0.0590                      | 1.65 ± 0.0510                           | 0.000897                |





**Supporting Information Table S8:** Top performing GNRs in a second cohort of lung cancer patients vs. age and gender-matched nominally healthy individuals. Serum rather than EDTA plasma was employed in this sample set. GNRs with 3-GalNAc as the denominator are greyed-out as they may simply indicate smoking status (Table 3).

|                               | <b>Lung Cancer (n = 16) vs. Healthy (n = 16)</b> | <b>Trend in Cancer</b>               | <b>Intra-Assay Precision</b> | <b>Inter-Assay Precision</b> |
|-------------------------------|--|--------------------------------------|------------------------------|------------------------------|
| <b>Glycan Node Ratio</b>      | <b>ROC AUC ± SE</b>                              | <b>(Increased or Decreased, I/D)</b> | <b>(%CV)</b>                 | <b>(%CV)</b>                 |
| 3-Gal/3-GalNAc                | 0.977 ± 0.026                                    | I                                    | 5.28                         | 8.28                         |
| t-Gal/2,4-Man <sup>a</sup>    | 0.922 ± 0.031                                    | D                                    | 7.06                         | 7.38                         |
| 2,4-Man/3-GalNAc <sup>a</sup> | 0.922 ± 0.043                                    | I                                    | 7.76                         | 11.97                        |
| 6-Gal/3-GalNAc <sup>a</sup>   | 0.918 ± 0.042                                    | I                                    | 5.29                         | 9.56                         |
| 2,4-Man/4,6-GlcNAc            | 0.914 ± 0.038                                    | I                                    | 8.95                         | 12.0                         |
| 2-Man/2,4-Man <sup>a</sup>    | 0.906 ± 0.037                                    | D                                    | 6.08                         | 8.93                         |
| 3,6-Man/3-GalNAc              | 0.910 ± 0.045                                    | I                                    | 3.83                         | 10.94                        |
| t-Gal/6-Gal <sup>a</sup>      | 0.887 ± 0.052                                    | D                                    | 2.34                         | 3.76                         |

<sup>a</sup> GNR overlaps with the top 12-performing GNRs in the Lung Cancer in Central and Eastern Europe cohort.

**Supporting Information Table S9:** Top performing GNRs in a cohort of colorectal cancer patients vs. age and gender-matched nominally healthy individuals. Serum rather than EDTA plasma was employed in this sample set.

|                            | <b>Colorectal Cancer (n = 10) vs. Healthy (n = 16)</b> | <b>Trend in Cancer</b>               | <b>Intra-Assay Precision</b> | <b>Inter-Assay Precision</b> |
|----------------------------|--|--------------------------------------|------------------------------|------------------------------|
| <b>Glycan Node Ratio</b>   | <b>ROC AUC ± SE</b>                                    | <b>(Increased or Decreased, I/D)</b> | <b>(%CV)</b>                 | <b>(%CV)</b>                 |
| 2-Man/6-Gal                | 0.969 ± 0.031  | D                                    | 4.76                         | 6.84                         |
| t-Gal/6-Gal <sup>a</sup>   | 0.969 ± 0.031  | D                                    | 2.34                         | 3.76                         |
| t-GlcNAc/3,4-GlcNAc        | 0.938 ± 0.018  | D                                    | 9.88                         | 15.5                         |
| t-Gal/2,4-Man <sup>a</sup> | 0.925 ± 0.036  | D                                    | 7.06                         | 7.38                         |
| t-Gal/2,6-Man <sup>a</sup> | 0.919 ± 0.041  | D                                    | 5.90                         | 9.82                         |
| t-Gal/3,6-Man <sup>a</sup> | 0.888 ± 0.062  | D                                    | 4.35                         | 5.69                         |
| 2-Man/2,4-Man <sup>a</sup> | 0.850 ± 0.063  | D                                    | 6.08                         | 8.93                         |

<sup>a</sup> GNR overlaps with the top 12-performing GNRs in the Lung Cancer in Central and Eastern Europe cohort.

**Supporting Information Table S10:** Top performing GNRs in a cohort of prostate cancer patients vs. age-matched nominally healthy males. Serum rather than EDTA plasma was employed in this sample set. As a common theme in these GNRs, 4-Glc (which, in serum may largely be derived from glycolipids) was found to increase.

| <b>Glycan Node Ratio</b> | <b>Prostate Cancer (n = 59) vs. Healthy (n = 75)</b> | <b>Trend in Cancer</b><br><b>(Increased or Decreased, I/D)</b> | <b>Intra-Assay Precision</b><br><b>(%CV)</b> | <b>Inter-Assay Precision</b><br><b>(%CV)</b> |
|--------------------------|--|--|--|--|
| Fuc/4-Glc                | 0.729 ± 0.044  | D  | 14.2   | 19.8   |
| t-Gal/4-Glc              | 0.714 ± 0.045  | D  | 11.0   | 17.7   |
| 4-Glc/3,4,6-Man          | 0.710 ± 0.044  | I  | 10.1   | 16.0   |
| 2-Man/4-Glc              | 0.688 ± 0.046  | D  | 11.3   | 17.9   |